7. Results of the Investigation of Tsho Rolpa

Among the potentially dangerous glacier lakes mentioned above, Tsho Rolpa glacier lake was intensively investigated for long term monitoring not only because it is growing rapidly and has an apparently greater likelihood of bursting but also because it is a typical moraine-dammed glacier lake in the Nepal Himalaya. The following aspects were studied.

- Geomorphological features of Tsho Rolpa,
- Interior dead ice sounding in the end moraine area,
- Meteorological conditions,
- Seasonal variation of the lake level and the amount of discharge
- Mass balance of lake water,
- Limnological studies of the lake, such as water temperature, suspended particles, its sedimentation and density stratification,
- Chemical composition of lake water and chemical background around the lake,
- Processes and rate of the present lake expansion,
- Present condition of the supra-glacial pond on the Trakarding glacier as an embryo of a glacier lake.

7. 1 Physical Setting of Tsho Rolpa

7. 1. 1 Location

Tsho Rolpa is located at an elevation of 4580 m a.s.l. on 27° 50' N ; 86° 28' E in the headwaters of the Rolwaling Khola, one of the tributaries of Tama Kosi which merges into Sun Koshi in Sapta Koshi water system as shown in Fig. 10. The direct aerial distance is 110 km east -northeast from Kathmandu. The north of the Rolwaling Valley is margined by Mt. Gauri Sankar range which runs from west to east and lies as the border between Nepal and Tibet, China. The Mt. Gauri Sankar (7146 m a.s.l.) is the highest mountain in the valley. The valley opens to the west and is connected to Khumbu Himal in the eastern fringe.

7. 1. 2 Longitudinal Cross Section along the River Downstream of Tsho Rolpa

As a typical example of a GLOF path along a river, the longitudinal cross section along Rolwaling Khola and Tama Kosi is shown in Fig. 11. The profile is drawn from Tsho Rolpa (4580 m a.s.l.) and is extended down to the confluence of Khimti Khola (590 m a.s.l.) where Khimti (Tama Kosi 2) Hydro-power Project has been initiated.

Rolwaling Khola runs 27 km along remarkably steep riverbed with an average inclination of 0. 12 to meet the confluence of Tama Kosi at an altitude of only 1390 m a.s.l. The gradient of the riverbed between Suri Dhoban and the confluence of Khimti Khola (590 m a.s.l) is comparatively gentle of the order of 0.016.

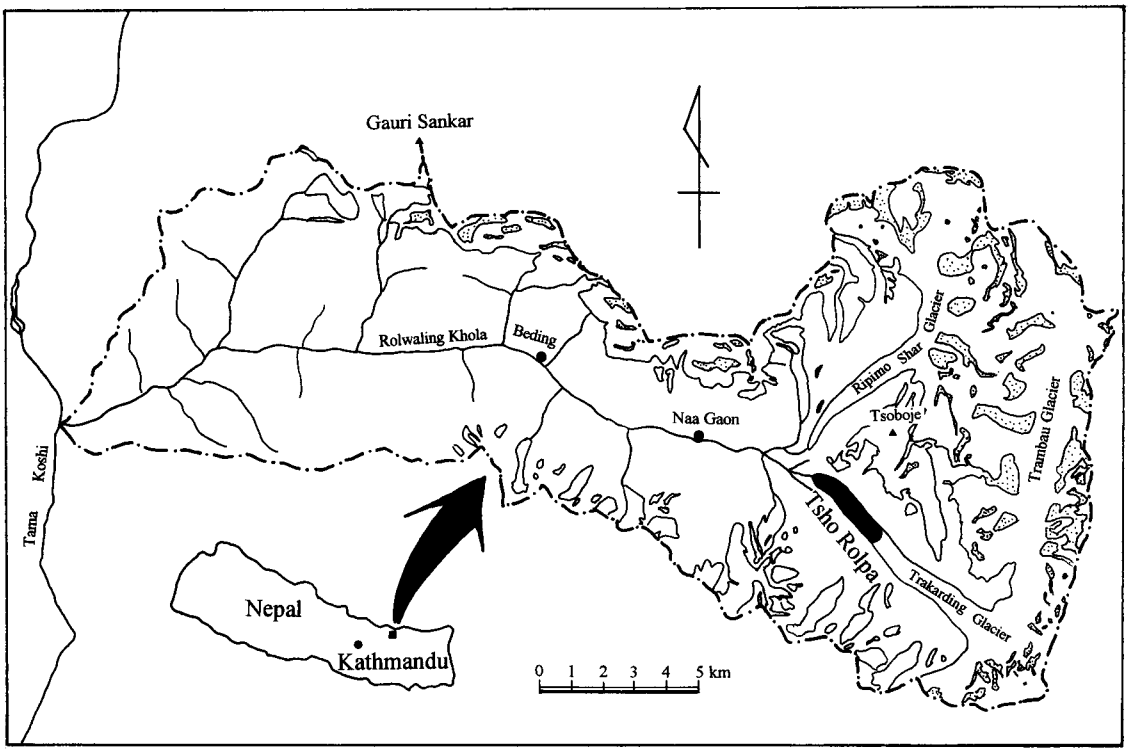

Fig. 10 : Location of Tsho Rolpa.

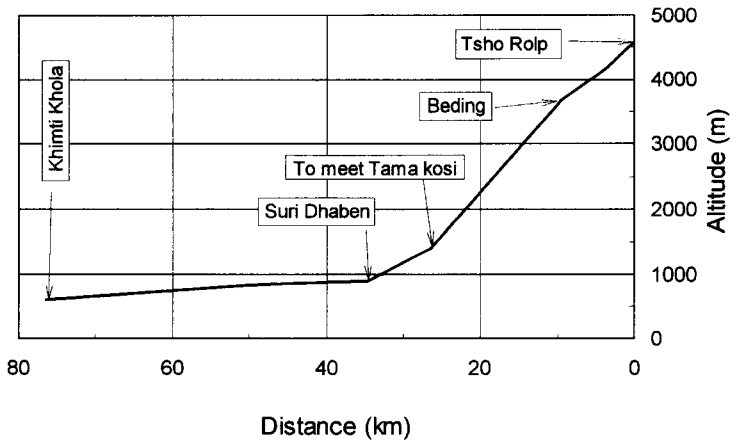

Fig. 11 : Longitudinal cross section along the Rolwaling Khola and the Tama Kosi.

7. 1. 3 Drainage Basin of the Lake

According to the topographical map (Schneider Map on a scale of 1 to 50,000), the drainage basin of Tsho Rolpa lies between 4580 m a.s.l., which is the lake level, and 6943 m of Mt. Tengi Ragi Ri, the highest peak. It is surrounded by 5000s m to 6000s m peaks in the fringe. Because of the altitude, the drainage basin is distinctively decorated with snow and glaciers as shown in Fig. 12.

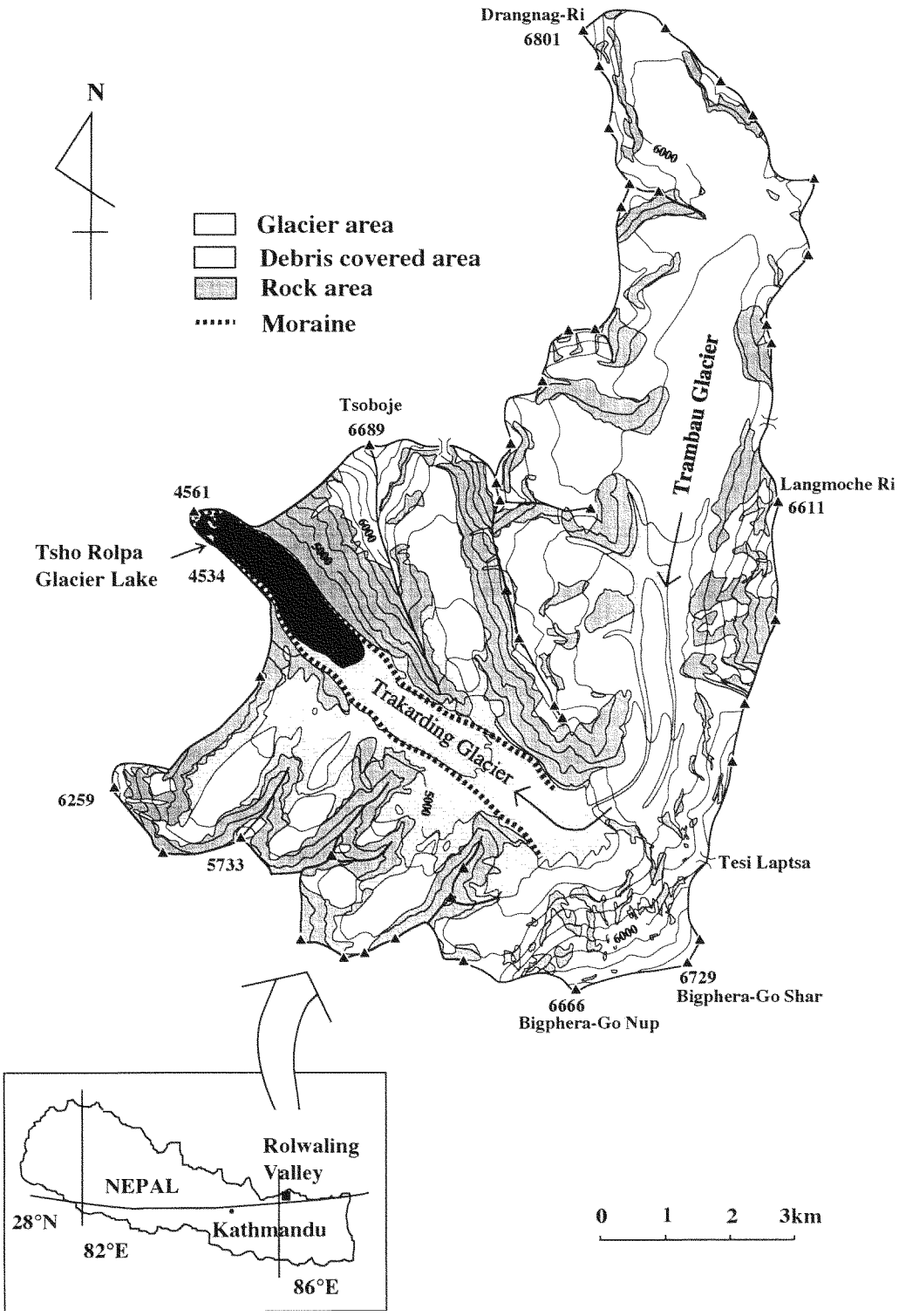

Fig. 12 : Drainage basin of Tsho Rolpa.

The compositions of the surface structure are shown in the figure. Altitudinal distribution of the areas for each composition of the surface structure is tabulated in Table 5 ; 55.3% and 16.5% of the total basin area of 77.6 km² were covered with debris free glaciers and debris covered glaciers, respectively. Only 26.5% is occupied by the bare rock surface. The area of Tsho Rolpa glacier lake, 1.39 km², occupies 1.7% of the basin area. The large ratio of the glacier area to the basin area indicates that meltwater of snow and ice is essentially important for the source of water supplied into the lake.

Table 5 : Altitudinal distribution of the Tsho Rolpa drainage basin.

( ) in %

Range of Altitude (m)		Area (km²)				
			debris free	debris covered		total
from	to	rock	glacier	glacier	lake	
4580	5000	1.16	0.40	9.00	1.36	11.92
		(9.74)	(3.39)	(75.50)	(11.41)	
5000	5400	5.57	6.30	2.72		14.60
		(38.18)	(43.16)	(18.64)		
5400	5800	7.81	15.71	1.09		24.61
		(31.75)	(63.82)	(4.43)		
5800	6200	4.21	16.25	0.00		20.47
		(20.58)	(79.40)	(0.00)		
6200	6600	1.74	3.79	0.00		5.52
		(31.47)	(68.59)	(0.00)		
6600	6943	0.03	0.41	0.00		0.45
		(7.34)	(92.22)	(0.00)		
	total	20.53	42.87	12.81	1.36	77.57
		(26.47)	(55.26)	(16.52)	(1.75)	(100)

7. 1. 4 End Moraine-dam

As shown by the cover photograph and Photo 14, Tsho Rolpa has been formed on the tongue of Trakarding glacier, one of the typical debris covered glaciers in the Himalaya. The lake is dammed by the end moraine as shown in Photo 23. The moraines looks quite fresh with no vegetation on them and are constituted of very loose debris carried by the glacier. The horseshoe -shaped moraine was formed during the Little Ice Age which happened a few hundred years ago when Trakarding glacier actively flowed down to the end moraine position. The height of the moraine-dam is 150 m from the riverbed of Rolwaling Khola and the inclinations of the outer slope are 30/100 at the upper part and 15/100 at the lower part. The lateral moraines are extremely loose and steep toward the lake. As such, continual collapses could occur into the lake as shown in Photo 24.

The moraine-dam is akin to one of those poorly constructed rock-fill dams composed of unconsolidated debris. Therefore, the dam is very unstable. As stated in the next Chapter, dead ice mass is contained in the end moraine and beneath the lake. Moreover the moraine is possibly frozen except for a few meters in the surface layer though there are no clear data. The ice masses and frozen condition of the moraine may endure the great hydro-pressure of the lake water.

Photo 23 : End moraine of the Trakarding glacier, about 150 m in height.

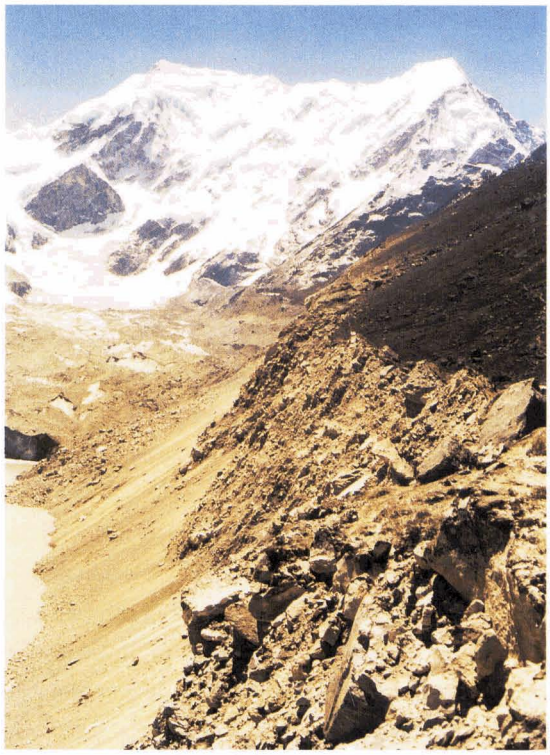

Photo 24 : Left lateral moraine with the loose and steep slope ; the end moraine of an unnamed glacier being also seen in the photo.

7. 1. 5 Upstream End of the Lake

The upstream end of the lake contacts the Trakarding glacier. The cliff-shaped terminus collapses periodically by calving so that, sometimes, icebergs are found as seen in Photo 25. The glacier retreats year after year by calving. This means that the lake is expanding upstream not by melting but by calving. The glacier is covered by thick debris of around 30 to 50 cm in depth except for the spots of spoon-cut shaped bare ice as seen in the figure. These features are common on the debris-covered glacier tongue in the Nepal Himalaya.

Photo 25 : Cliff-shaped glacier terminus contacting with the lake ; the glacier being covered with thick debris except the spots of spoon-cut shaped bare ice.

7. 1. 6 Shape of the Lake Basin

The shape of the lake basin was already shown in Fig. 6-c and is presented here again in Fig. 13 with valuable points, which will be conveniently referred to in Section 7. 5. The lake depth was first observed in February 1993. The preliminary results were presented in WECS Report (Mool et al., 1993). In February 1994 the measurements of lake depth were continued to obtain more detailed configuration of the lake basin. The bathometric map was improved using enough depth data (Kadota, 1994).

The surface area and volume of stored water have also been reassessed as 1.39 km^2 and 76.6 million m^3, respectively as already shown in Table 3. The relationships between the lake area and depth, and between cumulative volume of lake water and depth are respectively shown in Fig. 14 -a and -b. For lowering the lake level, for example by 20 m, lake water of about 25,000 m^3 would have to be drained out, which would cause the lake area to decrease to 1.05 km^2. As seen in the bathometric map of downlake area near the end-moraine (Fig. 15) prepared by Modder and Olden (1995), the basin shape is rather complex in comparison with the basin shape of the main lake. If lake level decreases down only to 10 m, the shore line retreat remarkably and the moraine-dam becomes thick enough, especially in the left bank side of the lake.

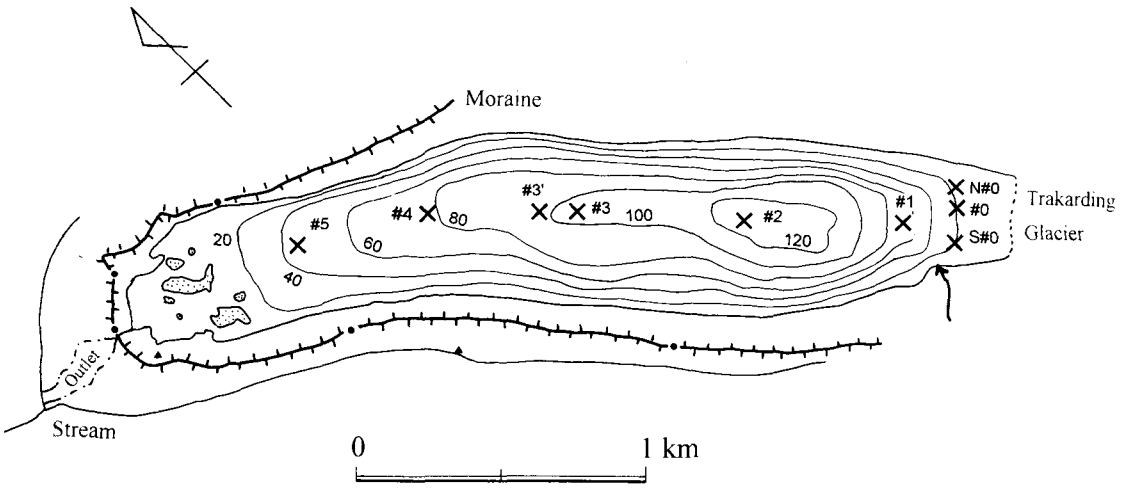

Fig. 13 : Bathometric map of Tsho Rolpa as of Feb. 1994 (after Kadota, 1994 ; modified). Arrow showing a small stream from an unnamed glacier in contact with the lake.
x : Points of limnological measurement.
● : Bench mark on the moraine ridge for the topographical survey.
▲ : Camping sites on the end moraine near the lake and in the valley out the left lateral moraine.

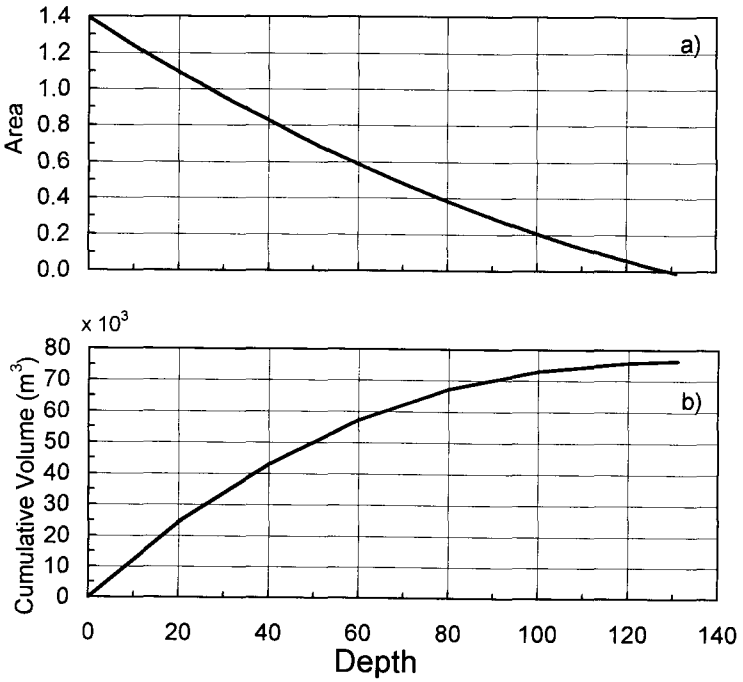

Fig. 14 : a) Relationship between lake area and depth.
b) Relationship between cumulative volume of lake water and depth.

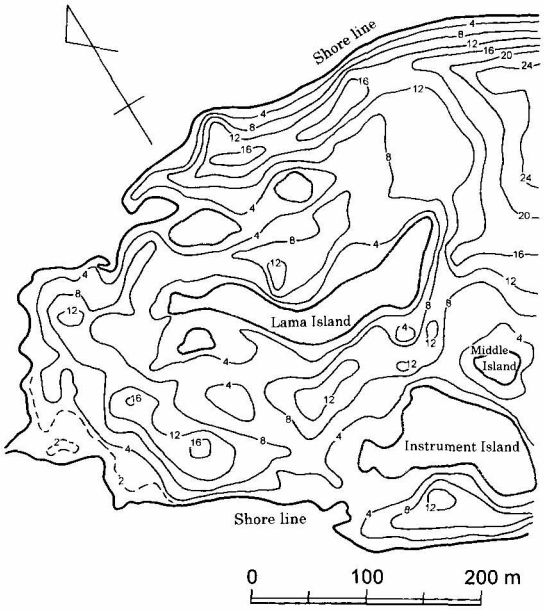

Fig. 15 : Bathometric map of downlake area near the end moraine (after Modder et al., 1995 ; simplified).

7. 1. 7 Islands in the Lake

The Islands are situated in the end part of the lake as exhibited in Fig. 13 and Photo 26, which

Photo 26 : Ice cored islands located at the downlake area of Tsho Rolpa.

are cored with dead glacier ice. With melting of cored ice, the islands are decreasing in height and will disappear into the lake in future.

7. 1. 8 Outlet of the Lake

Water supplied into the lake from the basin area of 77.6 km² is drained out through the outlet formed on the lowest part of the end moraine (Photo 27) throughout a year, even in winter season. At least four former outlets can be found on the moraine. Non uniform melting process of the cored ice in the moraine may have created the shifting outlets one after another. As a working outlet was

Photo 27 : Outlet stream on the end moraine viewing
a) from the foot of the end moraine ; b) from a helicopter.

changed to give place to newly created outlet, the absolute water level of the lake may have been shifted to the new level. In fact, shrubs are growing on a part of the moraine only beside the lake as seen in Photo. 28. The photograph shows the camp site for the lake study marked by ▲ in Fig. 16. Among the shrubs, those growing on the low level along just the lake shore have withered and died. The tree rings were counted to be 20 annual rings. On the other hand, the living ones at the relatively high level had 30 rings as of November, 1994 (Fujiwara and Gomi, 1995). This indicates that the lake level may have increased up to the dead tree level about 10 years ago.

Photo 28 : Shrub growing on the end moraine near the camping site.

7. 1. 9 Inflow Stream into the Lake

Only one visible small stream from the unnamed glacier in contact with the lake from the left bank side near the glacier terminus of Trakarding glacier can be recognized as only the source of surface water into the lake as shown by an arrow in Fig. 13. The end moraine of this unnamed glacier still contains the dead glacier ice under thick debris, which is now exposed at the terminus cliff as seen in Photo 29. Since the dead ice is exposed, violent melting occurs during the warm summer months. Meltwater has caused a small stream of some 20-40 L/s to pour into the lake as shown in Photo 30. No other water sources are found besides this surface stream. This means that almost all water in Tsho Rolpa drainage basin, such as meltwater of snow and ice as well as rainwater, must be absorbed and concentrate in the en-glacial drainage systems of the Trakarding glacier and pours into the lake through the en-glacial mouths (see Section 7.5.4.1) in the glacier terminus.

Photo 29 : Exposed ice body in the end moraine of an unnamed glacier bounding on the left side of the lake.

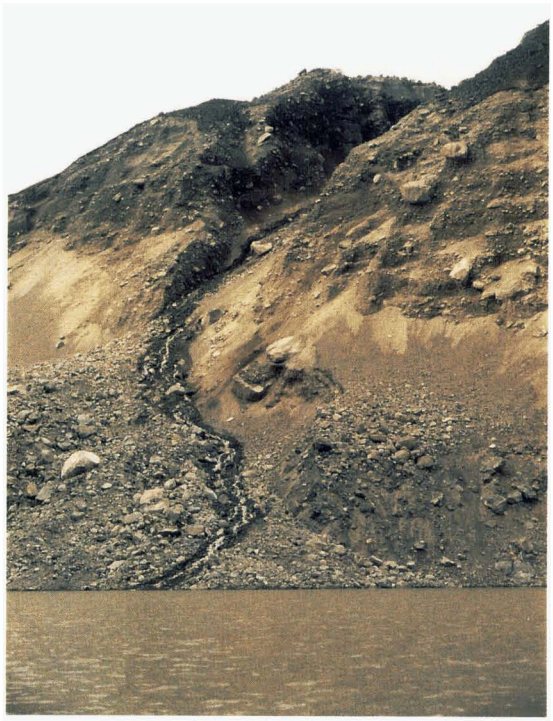

Photo 30 : Small stream of meltwater from the exposed ice shown in Photo 29.

7. 1. 10 Leakage

Seven leakage points were found on the outer slope of the end moraine as indicated by x-marks in Fig. 16. Leaking volume of water was measured to be of the order of 20 L/s at the largest leakage point. The level of the leakage point is some 50 m lower than the lake level, which corresponds to the water saturated area in the end moraine detected by the electric resistivity survey as mentioned in following Section 7.1.11. The other points of leakage release out a little water by volume. The development of such piping may weaken the end moraine structure.

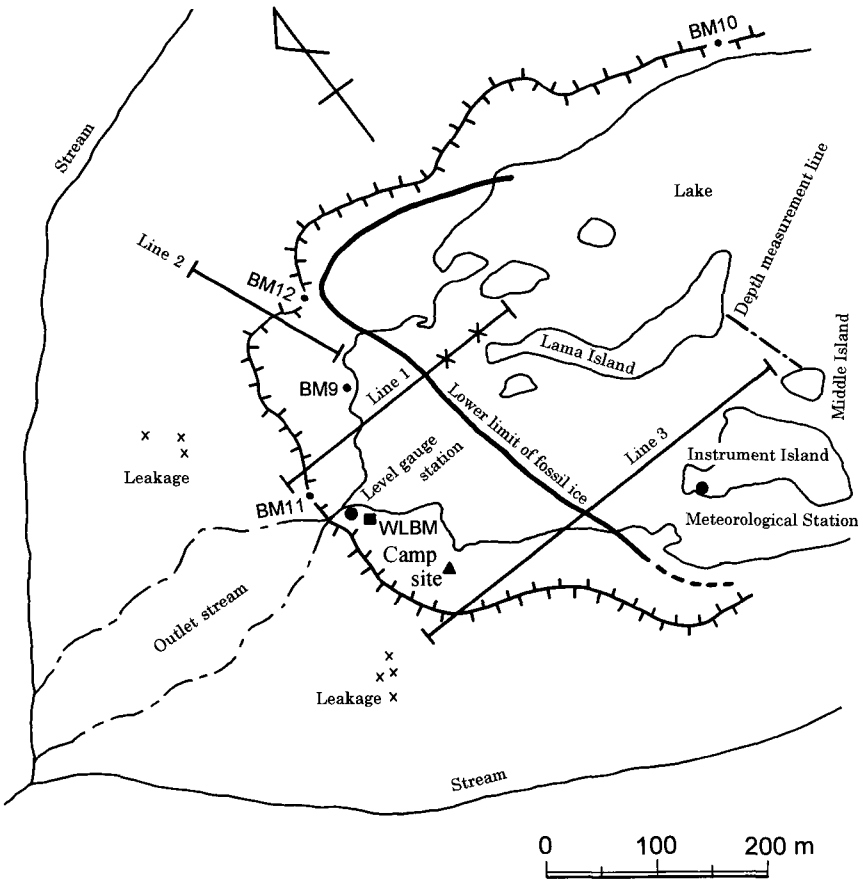

Fig. 16 : Map of the end moraine area.
Fine solid lines : Electrical resistivity survey line. Two marks, x, on the line 1 indicating the points of the vertical electric sounding.
Thick solid line : Most downstream limit of the ice cored area.
Dashed line : Depth measurement line between Lama Island and Instrument Island.
Chained line : Ridge of the moraine.
● : Position of the meteorological station and level gauge station.
■ : Water level bench mark.
▲ : Camping site.
x : Leakage point.

7. 1. 1 1 Dead Ice in the End Moraine Area

The most essential countermeasure to prevent the outburst flood of a glacier lake is to decrease the water level of the lake by making a deep enough breach in the moraine-dam not to allow overtopping of lake water. It will have the effect of diminishing the hydrostatic pressure against the moraine-dam. Furthermore even if the moraine-dam breaks, less amount of released water causes a relatively small flood so that considerably less damage may be expected.

Excavation of a breach in the moraine-dam may expose the interior ice body in the moraine. Once the ice body is exposed, strong solar radiation accelerates its melting, which results in the end moraine structurally to weaken and cause a spontaneous moraine-dam break by which a GLOF may be triggered. It is clear that the inner structure of an end moraine should be investigated before conducting any civil-engineering treatment to the moraine-dam.

For finding the depth and location of the ice body buried in the end moraine area, the Electric -Exploration Resistivity Method was applied in the post-monsoon season of 1994 (Kita, 1995). The method can provide us the profile of the electric resistivity (ER) in the interior of the moraine. Since materials have their own ER-value we can estimate and identify the material on the basis of the measured ER-value. Since ice is one of the good electric insulators, the ER-value should be very high among the materials of the end moraine area consisting of such materials as debris, bedrock, water and ice. The ER-values were measured in situ as 4,000 to 8,000Ω-m for the unsaturated moraine with water, 2000 to 4000 Ω-m for the saturated moraine and 500 to 1,000 Ω-m for water.

The surveyed points and lines are shown on the map of the end moraine area as illustrated in Fig. 16. First, the depths of ice mass were determined at two points on the lake near Lama Island marked by (x) on the survey line 1 in Fig. 16 by means of the Vertical Electric Sounding (VES). Then one-dimensional vertical distribution of ER-value can be obtained by VES method. The layer beneath 4 to 6 m from the surface showed a very high ER-value of more than 10,000 Ω-m. This indicated that ice mass exists just near the surface, only 4-6 m in depth, which means that the thickness of debris can be assumed to be 4-6 m. The meteorological station, water level gauge station and other important spots are presented in Fig. 16.

Next, cross sectional profiles of ER-values were obtained by means of the 2-Dimensional Electric Profiling along three survey lines 1 (150m in length), 2 (250m) and 3 (360m) as shown in Fig. 16. This method allows to detect a more detailed cross section of ER-values in the relatively wide area along the survey line than the VES method. The structure of the end moraine estimated by the cross sectional profile of ER-value is shown in Fig. 17. At some points 100 m far from the shore line in the survey lines 1 and 3, high ER-value more than 10,000 Ω-m were detected, which shows the presence of ice mass at a depth of 5 to 10 m under the lake bottom.

It was confirmed that dead ice mass is contained in the vicinity of the end moraine area of Tsho Rolpa.

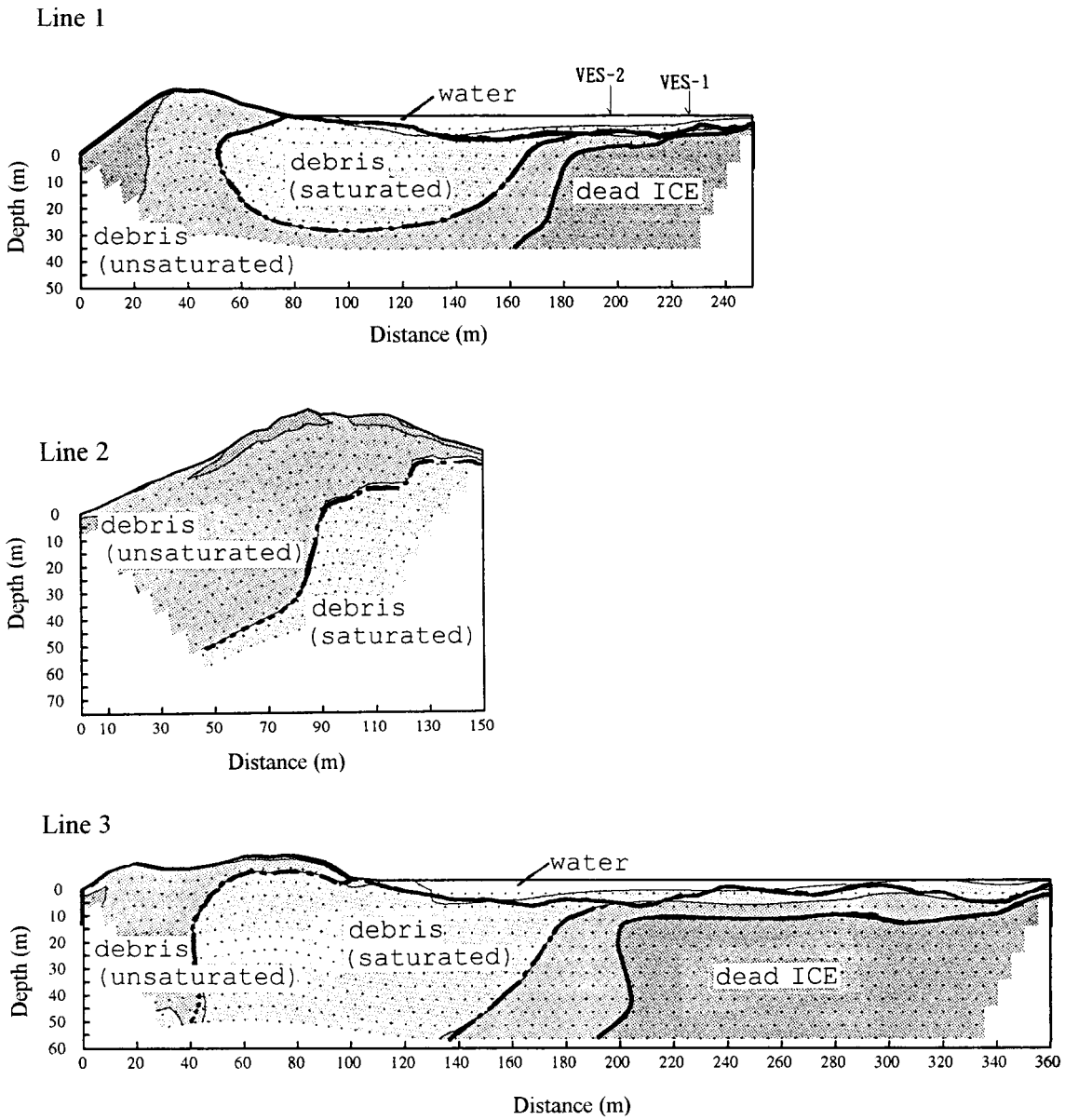

Fig. 17 : Internal structure of the end moraine area along three survey lines shown in Fig. 16 (After Kita, 1995 ; modified).

7. 2 Possible Risks for Tsho Rolpa GLOF

As regards the internal triggers for Tsho Rolpa GLOF, the existence of two kinds of triggers are identified. One is the possibility of a slope collapse and the other is an ice avalanche. As shown in Photos 29 and 30, the ice-cored end moraine of the unnamed glacier contacts with the lake. Whole the features are shown in Photo 31. A slope collapse of this very steep moraine with huge amount of mass may trigger the lake-burst. Hanging glaciers as shown in Photo 32 on the lake side slopes of Mt. Tsoboje (6689 m a.s.l.) in the right bank have a possibility of generating huge ice avalanches. Since ablation-valley in the right bank is completely buried by debris falling down from these steep slopes of Mt. Tsoboje, the avalanche directly falls down into the lake. An earthquake should also be considered as an external trigger contributing to lake-burst.

As mentioned in previous Section 7. 1. 10, there are several leakage points in the end moraine (x marks on Fig. 16). The development of conduits and continuous melting of the dead ice can weaken the end moraine. Thus, the other possibility of moraine-dam break is a sliding and/or a collapse of the end moraine spontaneously due to the piping and melting of the cored ice. Nobody can scientifically predict the timing of the burst, because it is fully unpredictable destruction phenomenon as the same as earthquakes.

Photo 31 : End moraine with the steep slope formed by an unnamed glacier.

Photo 32 : Hanging glaciers on the steep slope of Mt. Tsoboje in the right bank side of the lake.

7. 3 Meteorological Studies of Tsho Rolpa

The meteorological condition have been continuously observed by means of Aanderaa Automatic Weather Station (AWS-2700) from June 1993 to August, 1996 at the Instrument Island (4681 m a.s.l.) as shown by ● mark on the instrument island in Fig. 16 (Yamada, 1995).

Air temperature, humidity, wind direction and air pressure are measured at hourly intervals. The values of precipitation and global radiation are the integrating values during one hour. The rainfall sensor of bucket type has a catchment funnel with a precise 200 mm diameter orifice. Solid precipitation during winter are not fully reliable. Precipitation by snow may be underestimated. Wind speed sensor has two output signals, average wind speed and wind gust i.e. maximum wind speed during the sampling interval of one hour.

Monthly values and the extreme values of the meteorological elements are tabulated in Table 6. Maximum and minimum values indicate respectively the extreme hourly values during the month in Table 6.

Table 6 : Monthly values of the meteorological elements ; maximum and minimum values indicating respectively the extreme hourly value during the month. "From 8th Jun '93" and "To 19th Sep '93" meaning the data available only 8-30 Jun., 1993 and 1-19 Sep., 1993, respectively.

		Temperature ℃			Precipitation mm			Humidity %			Solar Radiation W/m²			Ave. WS m/s			Max. WS m/s			Air Pressure hPa		
		Ave.	Max.	Min.	Total	Max.	Min.	Ave.	Max.	Min.	Ave.	Max.	Min.	Ave.	Max.	Min.	Ave.	Max.	Min.	Ave.	Max.	Min.
From 8th	Jun '93	4.6	10.7	0.6	69.0	4.5	0.0	94	99	60	306	1672	0	2.2	6.1	0.0	4.7	12.5	0.9	587	590	584
	Jul '93	5.4	14.6	2.6	71.0	3.5	0.0	96	99	29	266	1687	0	2.1	6.3	0.1	4.3	11.0	0.6	588	591	585
	Aug '93	5.3	11.2	0.4	143.5	13.0	0.0	97	100	70	219	1657	0	1.7	5.5	0.1	3.8	9.3	0.6	588	591	584
To 19th	Sep '93	3.4	10.2	0.0	71.0	2.5	0.0	96	99	55	210	1607	0	1.7	5.3	0.1	3.8	9.0	0.6	589	592	587
	Oct '93	-	-	-	-	-	-	-	-	-	-	-	-	-	-	-	-	-	-	-	-	-
	Jan '94	-	-	-	-	-	-	-	-	-	-	-	-	-	-	-	-	-	-	-	-	-
From 21st	Feb '94	-7.3	6.4	-12.7	0.0	3.5	0.0	51	99	8	294	1741	0	2.5	6.4	0.1	8.0	14.9	1.2	580	590	580
	Mar '94	-3.8	11.7	-14.6	30.5	5.0	0.0	63	98	0	327	1662	0	2.3	9.8	0.4	6.3	32.8	1.2	583	587	579
	Apr '94	-3.6	6.4	-12.7	34.0	3.5	0.0	72	99	8	314	1714	0	2.1	6.4	0.1	5.3	14.9	1.2	585	590	580
	May '94	1.1	6.8	-4.8	30.5	4.5	0.0	86	99	15	364	1881	0	2.4	6.1	0.0	5.2	12.8	0.0	587	590	582
	Jun '94	4.9	10.5	-0.5	46.0	4.0	0.0	93	99	23	332	1652	0	2.3	5.9	0.0	4.9	10.4	0.0	586	589	584
	Jul '94	5.5	12.9	2.1	104.0	4.5	0.0	96	100	64	287	1786	0	2.5	6.9	0.0	4.9	11.3	0.6	587	591	584
	Aug '94	5.1	11.0	1.9	109.0	4.0	0.0	97	100	74	240	1791	0	2.2	6.2	0.0	4.5	10.1	0.6	589	591	587
	Sep '94	4.0	3.8	0.7	55.0	3.0	0.0	93	100	32	254	1557	0	2.3	6.9	0.1	4.6	10.7	0.9	590	593	585
	Oct '94	0.0	9.3	-5.8	0.0	0.0	0.0	63	99	0	283	1264	0	2.3	7.1	0.3	4.8	11.3	1.2	589	593	585
	Nov '94	-6.0	4.0	-15.0	5.0	2.0	0.0	67	98	4	194	1284	0	2.2	6.9	0.0	4.6	20.3	0.0	587	593	580
	Dec '94	-5.4	7.1	-15.5	0.5	0.5	0.0	33	88	0	168	894	0	2.3	9.9	0.1	6.4	28.3	0.9	585	590	578
	Jan '95	-9.2	1.8	-2.1	6.5	1.5	0.0	39	86	0	162	991	0	2.4	6.6	0.3	7.1	20.6	1.5	582	587	576
	Feb '95	-8.3	2.4	-23.2	12.5	2.0	0.0	52	88	0	217	1377	0	2.4	6.8	0.0	6.9	18.0	0.0	581	588	574
	Mar '95	-4.4	8.7	-17.7	18.0	2.5	0.0	51	93	0	265	1363	0	2.5	6.9	0.0	7.0	11.0	0.0	585	590	579
	Apr '95	-2.6	5.8	-13.5	29.0	10.0	0.0	60	94	0	332	1638	0	2.5	7.7	0.2	6.0	13.1	2.1	586	591	581
	May '95	2.6	8.7	-5.0	28.0	3.0	0.0	75	97	17	356	1773	0	2.9	7.5	0.0	5.7	12.5	0.0	588	591	583
	Jun '95	5.4	10.3	2.6	76.5	6.0	0.0	82	93	40	251	1582	0	2.5	7.1	0.2	5.1	12.5	1.2	-	-	-
	Jul '95	5.3	10.9	0.8	196.0	6.0	0.0	82	88	42	231	1680	0	2.4	6.5	0.1	4.8	10.4	0.9	-	-	-
	Aug '95	5.0	10.4	1.6	215.0	6.5	0.0	81	87	39	227	1689	0	2.3	6.6	0.0	4.5	11.0	0.6	-	-	-
	Sep '95	3.7	10.3	0.0	97.0	3.0	0.0	80	87	28	215	1596	0	2.3	6.6	0.1	4.5	10.4	0.9	-	-	-
	Oct '95	-3.6	4.6	-7.9	8.0	5.0	0.0	56	87	0	246	1275	0	2.3	7.2	0.0	4.8	12.8	0.0	590	593	587
	Nov '95	-7.5	1.2	-13.3	7.0	3.0	0.0	46	90	0	190	1028	0	2.1	6.6	0.0	4.7	11.3	0.0	587	592	581
	Dec '95	-9.5	-1.0	-20.5	0.5	0.5	0.0	50	91	12	158	963	0	2.1	6.6	0.3	5.9	15.5	1.5	585	593	581
	Jan '95	-10.3	-2.6	-20.6	3.5	0.5	0.0	44	93	12	180	1010	0	2.9	8.9	0.6	8.8	32.5	2.1	582	594	577
	Feb '96	-11.5	-3.8	-27.9	10.0	4.0	0.0	63	94	21	224	1447	0	2.7	9.8	0.0	6.9	21.8	0.0	583	593	577
	Mar '96	-8.1	4.0	-16.3	34.0	7.0	0.0	65	97	7	298	1456	0	2.7	9.9	0.0	6.9	29.8	0.0	583	590	576
	Apr '96	-7.0	6.3	-15.8	25.5	4.5	0.0	70	96	10	345	1587	0	2.5	6.9	0.0	5.6	16.1	0.0	586	591	580
	May '96	-3.7	5.7	-9.1	22.0	6.5	0.0	72	94	0	357	1801	0	2.8	7.5	0.0	6.0	15.8	0.0	586	590	582
	Jun '96	3.5	9.6	-3.0	-	-	-	80	89	53	256	1652	0	2.6	6.9	0.0	5.2	13.4	0.0	587	592	583
	Jul '96	5.4	10.8	2.6	-	-	-	82	86	62	205	1489	0	2.1	6.3	0.0	4.3	10.4	0.6	587	591	585
	Aug '96	4.8	9.8	0.8	-	-	-	80	86	48	206	1647	0	2.2	6.3	0.0	4.3	10.4	0.6	589	592	586
To 13th	Sep '96	3.7	9.3	0.5	-	-	-	81	86	51	209	1484	0	2.2	5.9	0.1	4.3	10.1	1.2	590	591	588

7. 3. 1 Air Temperature

Seasonal variation of daily mean air temperature is shown in Fig. 18. Daily mean air temperature keeps above 0°C during the mid-May to the mid-October and below 0°C during the mid-October to mid-May of next year. As seen in the figures, air temperature is almost constant around 5-6°C during the monsoon season ; large periodic fluctuation with the cycle of about 10 days characterizes the dry season from November to May. Annual average air temperature in 1994 and 1995 are respectively -1.2 and -1.9°C. As seen in Table 6, the warmest month is mostly July with monthly average of 5.3-5.5°C in 1993-1996 ; the coldest is January or February with -9.2°C in Jan., 1995 and -11.5℃ in Feb., 1996 ; the maximum and the minimum hourly values of air temperature during three years are, respectively, +14.6°C on 6 Jul., 1993 and -23.2°C on 16 Feb., 1995.

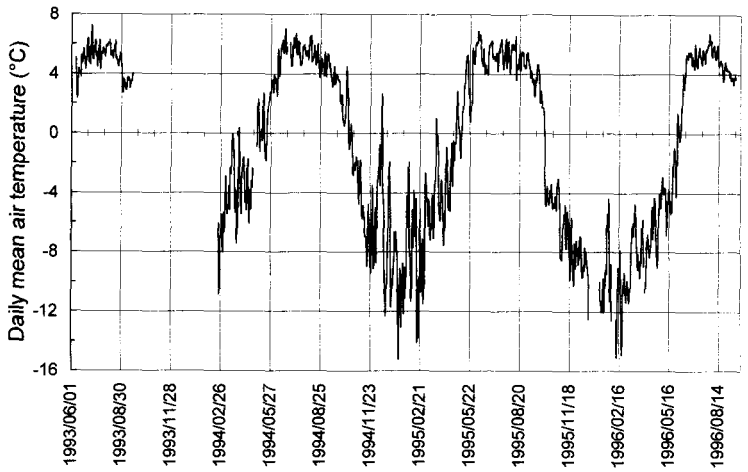

Fig. 18 : Seasonal variation of daily mean air temperature.

7. 3. 2 Precipitation

Daily amount of precipitation is shown in Fig. 19. Though appreciable precipitation occurs even in the dry season from January to May, 64 to 72 % of annual precipitation are concentrated in the monsoon season from the mid-June to the mid-September in 1994 and in 1995, respectively. The annual precipitation is recorded as 414.5 mm in 1994 and 694.0 mm in 1995. The maximum monthly precipitation of 243.5 mm occurred in August, 1993. The localized heavy rainfall did not occur during the observed period because the maximum hourly precipitation was recorded as only 13.0 mm in August, 1993 as shown in Table 6.

7. 3. 3 Humidity

Daily mean humidity is shown in Fig. 20. Relative humidity data shows that this region belongs to the typical monsoon climate : Considerable high values and relatively small diurnal variation characterize the monsoon season form mid-June to mid-September. The maximum of monthly average is 97 % in August both in 1993 and 1994. Daily mean humidity rapidly decreases after the monsoon season from the end of September. December and January are the driest months in a year

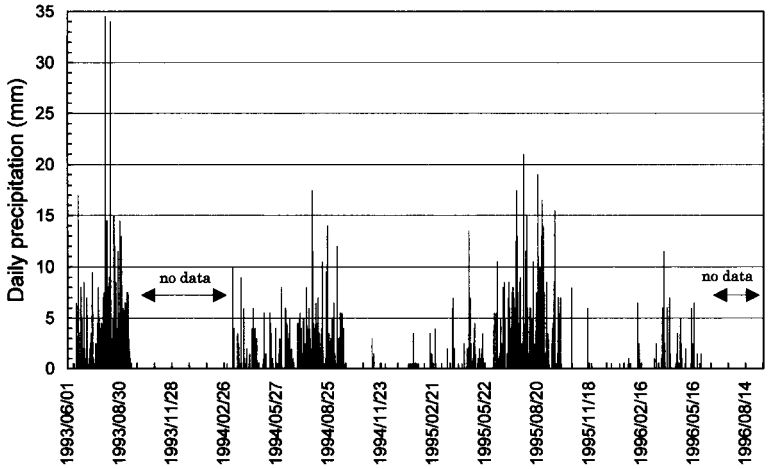

Fig. 19 : Seasonal variation of daily precipitation.

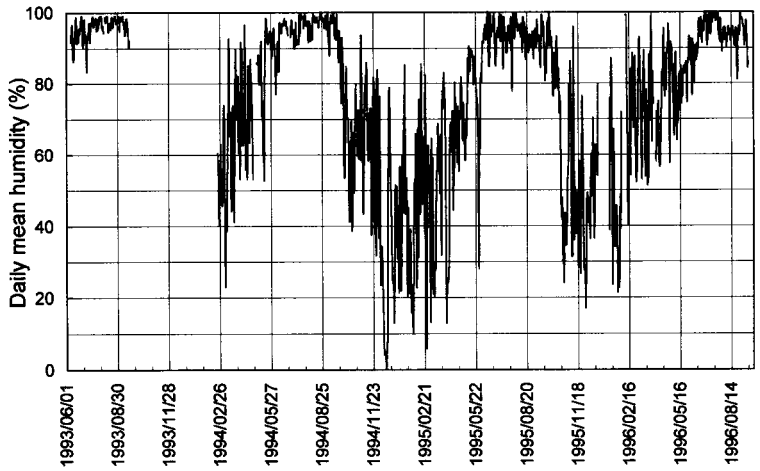

Fig. 20 : Seasonal variation of daily mean humidity.

with monthly average value of only 33-44 %, and tends to gradually increase to the next monsoon season. Dry season from the end of September to the end of May is characterized by large diurnal and daily variation.

7. 3. 4 Solar Radiation

Daily amount of solar radiation is shown in Fig. 21. The annual mean solar radiation is 269 W/m^2 in 1994 and 237.6 W/m^2 in 1995 which corresponds to 23.2 and 20.5 MJ/m^2/day, respectively. The solar radiation reaches a minimum in December/January ; the monthly mean of 158-180 W/m^2, while the maximum is observed in May just before the monsoon season with a value of 356-364 W/m^2 as shown in Table 6. The maximum hourly solar radiation was recorded of 454 W/m^2 (39.2 MJ/m^2/day) on May, 1994.

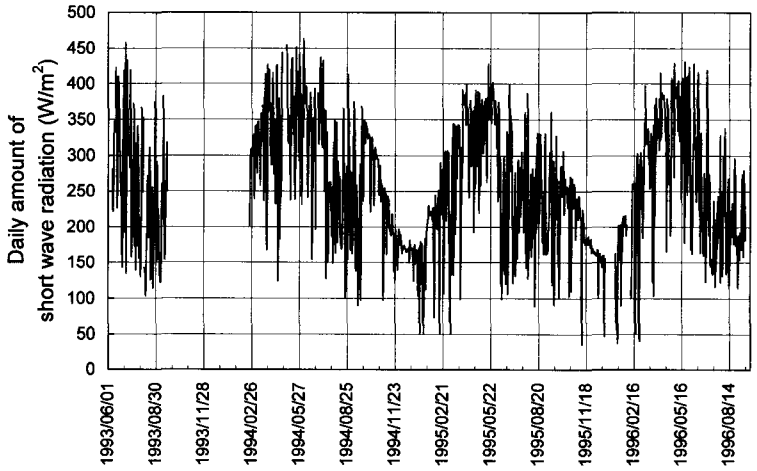

Fig. 21 : Seasonal variation of daily amount of short wave radiation.

7. 3. 5 Wind Speed

Wind speed was measured for average and the maximum (gust) values during 1 hour interval as shown in Figs. 22-a and -b. Daily mean values are rather weak and quite stable at 1.7 to 2.9 m/s throughout a year and the annual average is only 2.1 m/s in 1994 and 2.4 m/s in 1995, respectively.

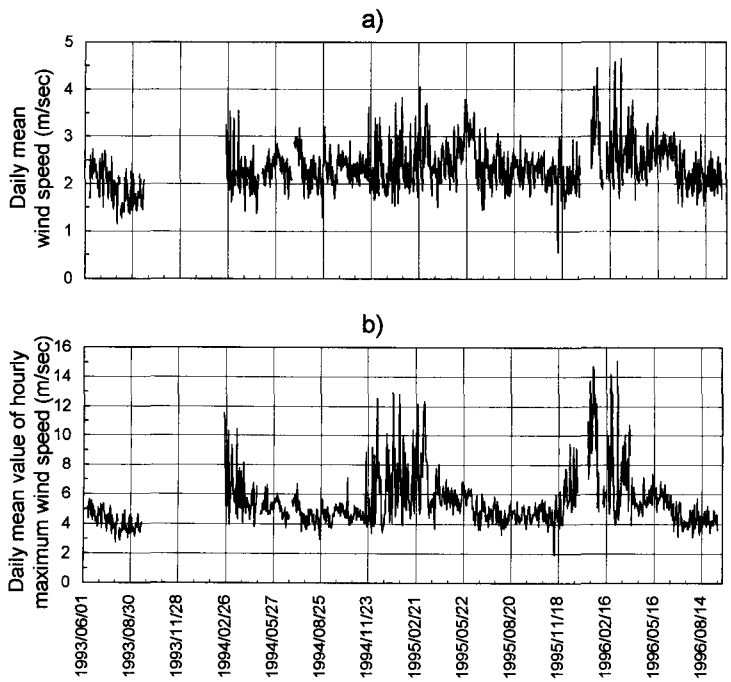

Fig. 22 : Seasonal variation of a) daily mean wind speed ;
b) daily mean value of hourly maximum wind speed.

The maximum wind speed is rather stable in the period from April to November at around 5 m/s but fluctuates considerably in the dry winter season from December to March as shown in Fig. 22-b. Strong gusts often occurred at more than 20 m/s in this dry season and the extreme value was recorded as 32.8 m/s on 17 March, 1994.

The periodic diurnal variation can be clearly seen throughout a year except winter season in December to February as shown in Figs. 23-a, b, c and d ; gentle and almost constant wind speed less than 2 m/s continues during the night in most seasons and a little bit more than 2 m/s during winter. Wind speed starts to increase at around 8 : 00 to 9 : 00 and reaches a daily maximum of around 5 m/s at 12 noon to 14 : 00 ; then gradually decreases and reaches again to the gentle and constant night wind at 18 : 00 to 20 : 00.

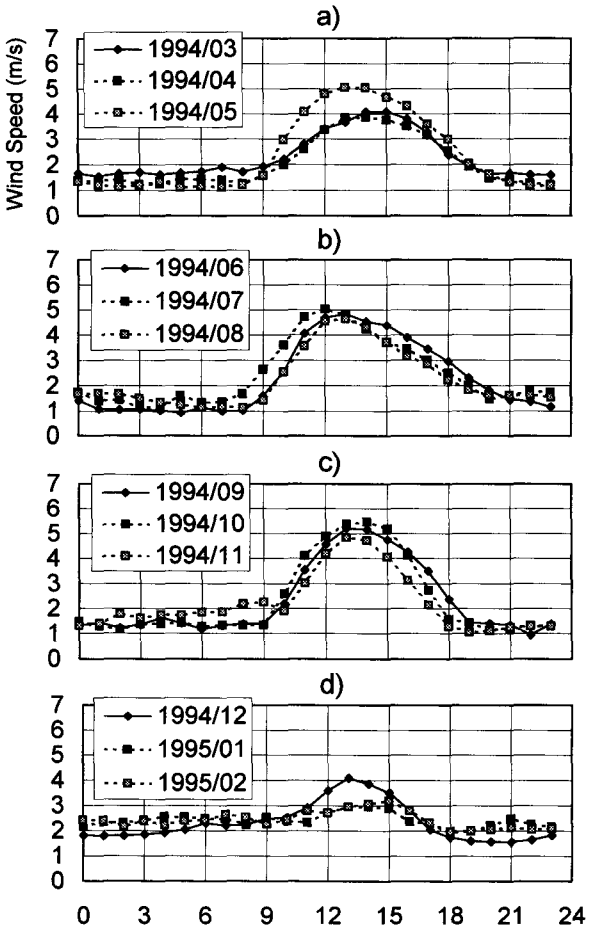

Fig. 23 : Diurnal variation of hourly mean wind speed monthly averaged :
a) March to May.
b) June to August.
c) September to November.
d) December to February.

7. 3. 6 Wind Direction

Wind at Rolwaling Valley is characterized by evident up-valley wind. As seen in Figs. 24-a, b, c, and d, wind in daytime at Rolwaling Valley corresponds to the up-valley wind in the direction of NW (315°). The axis of the valley is in NW to SE as seen in Fig. 12. The up-valley wind develops clearly from May to November (Fig. 24-a, b, c) and is obscured in winter from December to April (Fig. 24-d and -a). On the contrary, the down-valley wind in night is not clear. Direction of night wind is not down-valley direction of SE (135°) but mostly in between S to W ; only in winter season of December to April to be SE to S.

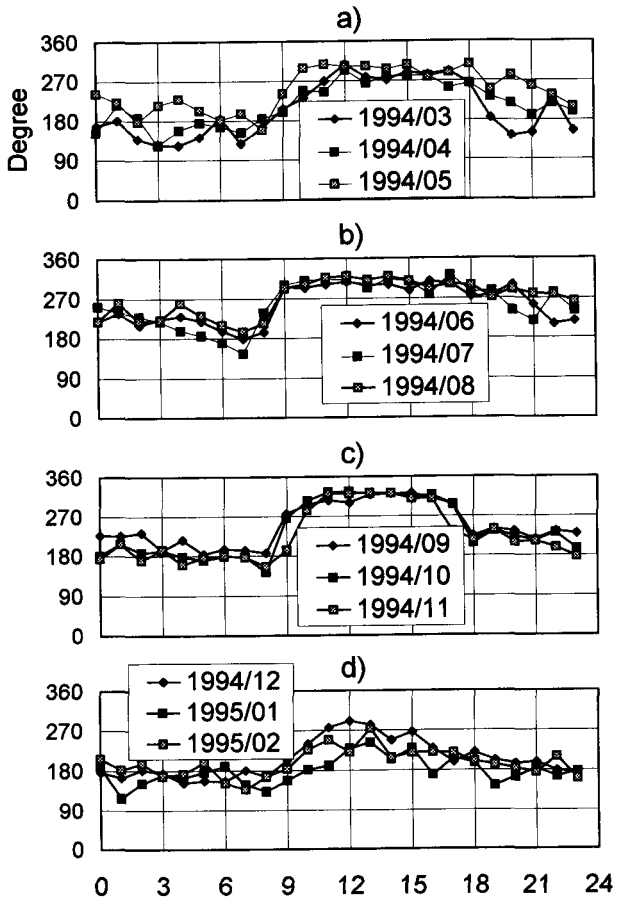

Fig. 24 : Diurnal variation of hourly mean wind direction monthly averaged :
a) March to May.
b) June to August.
c) September to November.
d) December to February.

7. 3. 7 Air Pressure

The annual mean air pressure at Tsho Rolpa (4580 m a.s.l.) is 585.8 hPa in 1994 and 585.5 hPa in 1995, respectively. Air pressure shows a seasonal fluctuation : Monthly minimum is 580-583 hPa in January/February and the maximum is 590 hPa in Septembers, 1994 and 1995. It also shows about 10 days periodic fluctuation as shown in Fig. 25 ; the amplitude of the periodic fluctuation is small during the monsoon season and large in dry season. Air pressure seasonally fluctuate in between 574 (hourly minimum) and 593 hPa (hourly maximum), which difference is only 19 hPa as seen in Table 6. Air pressure is surprisingly stable throughout a year. Air pressure shows a clear diurnal bi-peak variation.

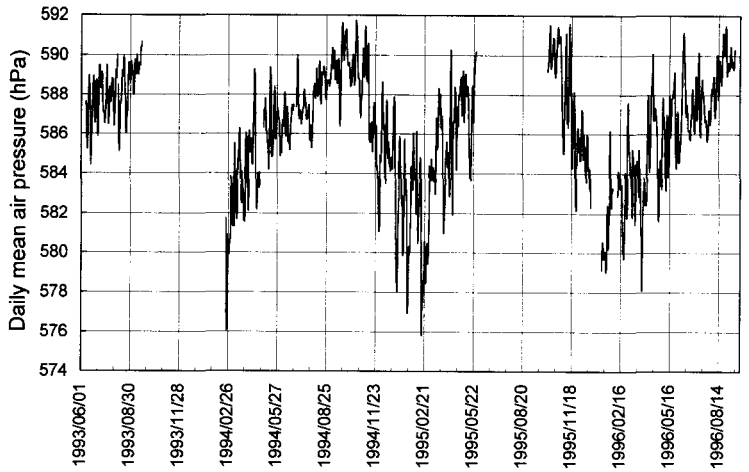

Fig. 25 : Seasonal variation of daily mean air pressure.

7. 4 Hydrological Studies of Tsho Rolpa

As already stated, the glacier lake Tsho Rolpa receives all meltwater and rainwater from the drainage basin of 77.6 km^2. Such water pouring into the lake overflows through the outlet cutting the end moraine. In order to obtain the hydrological features of the lake, the following hydrological elements such as water level and relationship between water level and discharge were observed.

7. 4. 1 Water Level

Water level was automatically and continuously measured at the interval of every 1 hour by using a pressure type water level gauge of the resolution of 1 mm (Yamada, 1996). Photo 33 shows the overlooking view of the outlet ; the bridge was temporally constructed for the discharge measurement ; a water level gauge was installed on the left bank just upstream of the bridge. The size of the stream is about 5 m in width and 2 m in depth at the deepest point. Water level was also measured manually in each field visit with reference to water level bench mark (WLBM) as shown by ■ mark in Fig. 16. The measurement aims at obtaining the seasonal variation of discharge through the outlet by using the observed relationship between water level and discharge.

Photo 33 : Overlooking view of the outlet. Level gauge being installed near a bridge temporally constructed.

The seasonal variation of diurnally averaged lake level referred to WLBM is shown in Fig. 26. The minimum water level of the base flow suddenly starts to increase in the beginning of the melting season at the early May and reaches the maximum level in July. After the rainy season, lake level decreases gradually and monotonously toward the minimum level realized in mid-March. Thus it is clear that the hydrological year of Tsho Rolpa drainage basin starts from mid-March. High water level is retained in the monsoon of 1995. This is coincident with high monsoon precipitation in 1995 as shown in Fig. 19. The monsoon in 1995 is more active than those in 1993 and 1994. Water level annually fluctuates in approximately 2 m between -132 cm (hourly minimum)

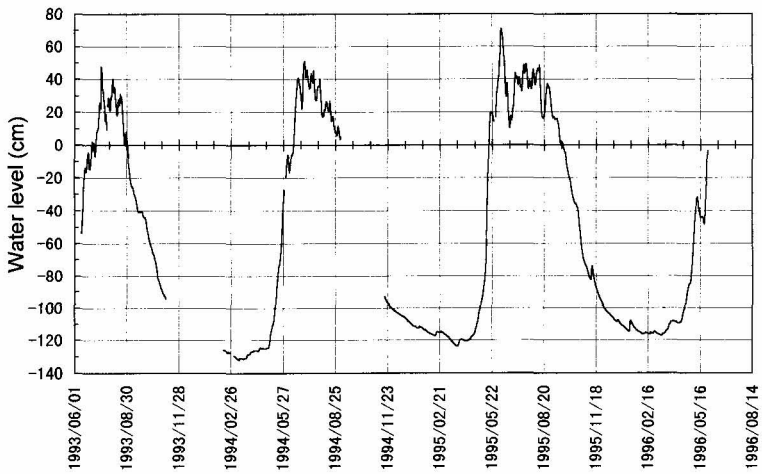

Fig. 26 : Seasonal variation of water level of the lake.

and +79 cm (hourly maximum). The hourly highest levels are of 65.5 cm on 17 July, 1993, 56.4 cm on 2 July, 1994 and 78.7 cm on 6 June, 1995 in the rainy season and the hourly lowest levels of -132. 3 cm on 12 March, 1994 and -123.9 cm on 23 March, 1995, -117.5 cm on 12 March, 1996.

Clear diurnal variations in the lake level are observed in the melting season as shown in Fig. 27 as an example. The diurnal variations characterize discharge from the drainage basin covered by snow and glacier. This is caused by the diurnal variation of meltwater supply into the lake : Snow and glacier melting are closely related to the diurnal variation of air temperature and solar radiation. After the melting season, the diurnal variation disappears.

Unexpected fluctuations of lake level sometimes happened due to the calving of the glacier terminus or sudden drainage of a supra-glacial pond into the lake. Usually the amplitude of the fluctuation was within±30 cm. The phenomena occurred at least once in each field visit of 1993 to 1996.

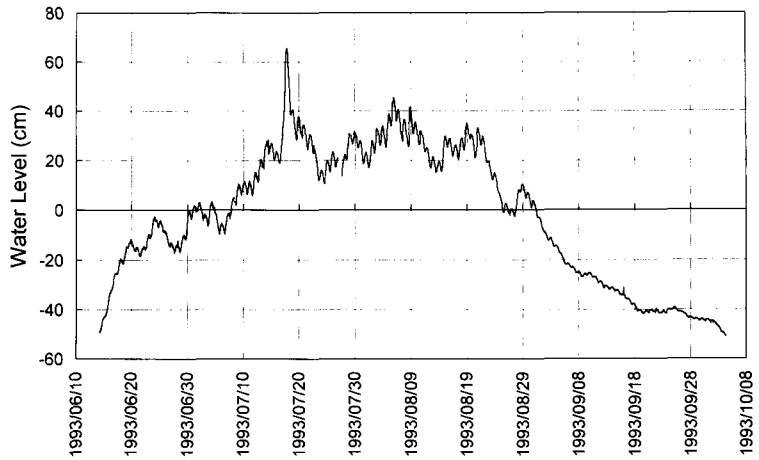

Fig. 27 : Water level clearly showing diurnal variation in the melting season.

7. 4. 2 Discharge

Discharge measurements were carried out by means of flow velocity measurement mainly during the field visits of July and November 1994 for obtaining the relationship between water level and discharge. A flow velocity sensor was attached to a steel rod. When discharge was at more than about 4 m^3/s, only flow velocity at the surface (V_S) was measured because the steel rod was not strong enough to stand the high flow velocity ; the average flow velocity was assumed as $0.88V_S$.

The relationship between water level and discharge is shown in Fig. 28. The empirical equation derived is :

$$Q = 4.9247\exp(0.0211h)$$

where Q is discharge in m^3/s and h is water level referring to WLBM in cm.

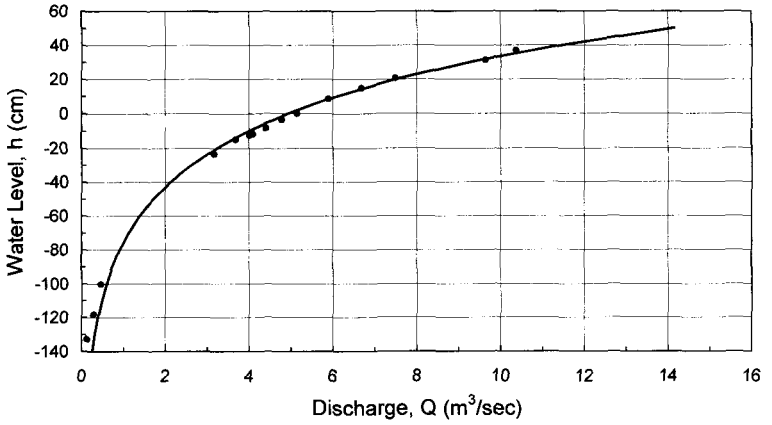

Fig. 28 : Relationship between water level (referring to water level bench mark) and discharge.

By using this equation, the water level is converted into discharge. The seasonal variation of daily mean discharge and daily runoff are shown in Fig. 29. The maximum discharge was 19.6 m^3/s on 17 July, 1993, 16.2 m^3/s on 2 July, 1994 and 25.9 m^3/s on 6 June, 1995 ; the minimum discharge was 0.30 m^3/s on 12 March, 1994, 0.36 m^3/s on 23 March, 1995 and 0.41 m^3/s on 12 March, 1996. The coefficient of river regime is only around 60, which is a rather small value compared to the large seasonal variation of precipitation. The annual amount of lake discharge is calculated to be 92.6 million m^3 from 15 March, 1994 to 14 March, 1995 and 128.9 million m^3 from 15 March, 1995 to 14 March , 1996, respectively ; the annual average discharge of 2.9 m^3/s in 1994-hydrological year and 4.1 m^3/s in 1995-hydrological year, equivalent to 3.2 mm/day in 1994 and 4.5 mm/day in 1995. This corresponds to the annual total runoff of 1193 mm in 1994 and 1661 mm in 1995.

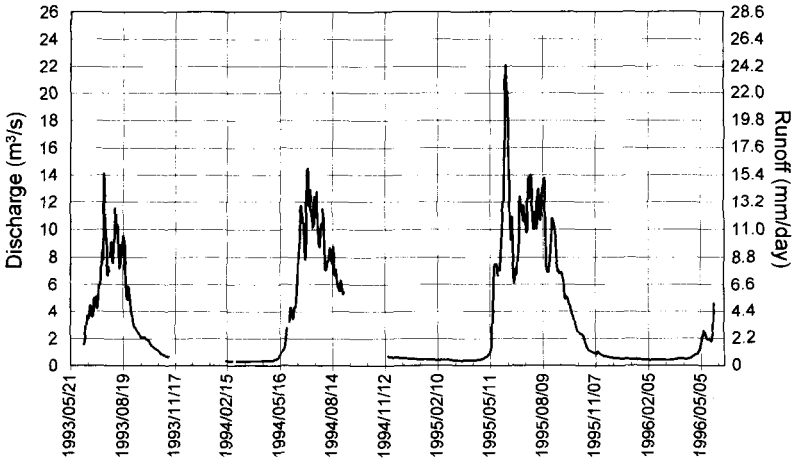

Fig. 29 : Seasonal variation of daily mean discharge and daily runoff.

Annual mass balance in the Tsho Rolpa drainage basin can be expressed by the following equation :

$$P = Q + E + \Delta G + \Delta S,$$

where P is the annual precipitation over the drainage basin ; Q is the annual amount of discharge through the outlet of the lake ; E is annual evaporation ; ΔG is the change in the glacier mass and ΔS is the change in the volume of stored water in the drainage basin. The value E is assumed to be nearly zero because of low temperature even in summer, and ΔS is also regarded as zero because of the period of one year. If the precipitation in 1994- and 1995- hydrological year of 424.3 mm and 696.5 mm, respectively, observed at the Meteorological Station (Section 7.3.2) are assumed as P, ΔG are calculated as 424 - 1193 = -769 mm in 1994 and -964 mm in 1995. These amount give the total annual loss of the glacier mass in the Tsho Rolpa drainage basin in 1994- and 1995-hydrological year. These values are too large for the glaciers even to suffer unusually large melting. P may be more than the observed precipitation, i. e. more precipitation may have occurred at the higher altitudes in the drainage basin.

7. 4. 3 Change of the Lake Level by Means of Artificial Drainage of Lake Water

Employing the data of an annual hydrograph at the outlet, the change of lake level due to an artificial draining out of the lake water is easily calculated. By interpolating discharge in the period between September and November, 1994, when the data was lacking, the daily mean discharge in one hydrological year is estimated as a typical and moderate annual hydrograph of the lake drainage. The hydrological year is defined as a period from 15 March, 1994 to 14 March, 1995 referring to the lowest water level. The lake level changes with lapse of time are shown in Fig. 30

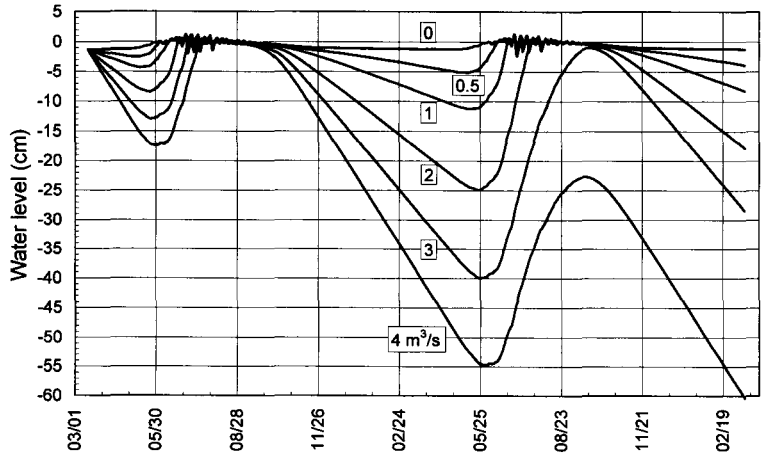

Fig. 30 : Lake level change with lapse of time in the cases of the artificial drainage amount of 0 (Natural), 0.5, 1, 2, 3, 4 m^3/s, respectively. The drainage starting from 15 March, the beginning of the hydrological year when the lake level is the lowest.

in the cases of the artificial drainage in 0 (Natural), 0.5, 1, 2, 3 and 4 m^3/s, respectively, which started from 15 March, the beginning of the hydrological year. The lake level decreases remarkably during the dry season when no rainwater and no meltwater are produced because of low temperature below freezing point. During the monsoon season, however, huge amounts of rainwater and meltwater are poured into the lake and the lake level quickly recovered from the end of May when melting starts. The lake level changes are calculated for two years. After the two years the fluctuation of lake level is repeated in the first five cases of the artificial drainage condition. Only in the case with a discharge of 4 m^3/s, the water level is not recovered exhibiting a quick decreasing trend.

7. 5 Limnological Studies of Tsho Rolpa

7. 5. 1 Thermal Condition of the Lake

7. 5. 1. 1 Vertical Profile of Water Temperature

To clarify the thermal structure of the lake, the vertical profiles of water temperature were observed during each field visit. The measurements were made at several points along an approximate center line in the longitudinal direction of the lake from near the end moraine to the proximity of the glacier terminus.

Seasonal variation of vertical temperature profiles at around the deepest point is shown in Fig. 31. Water temperature at the surface fluctuates from 6.0°C in summer to 0°C in winter. The seasonal

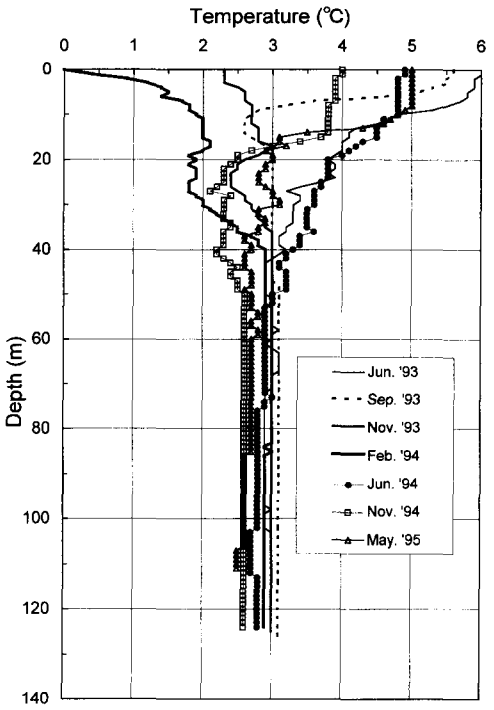

Fig. 31 : Seasonal variation of the vertical profile of water temperature at around the deepest point.

fluctuation gradually decreases in amplitude with increasing depth down to 50 m. Below this depth, the temperature seasonally fluctuates only within 2.6-3.1°C in spite of the maximum density of pure water being realized at around 4 °C. Tsho Rolpa is thus characterized by such a unique thermal structure as shown by the upper active layers in less than 50 m in depth and the deeper quasi -isothermal layer.

The dead ice beneath the lake bottom may not directly contact with lake water but with the lake sediment putting on the debris. The surface temperature of the sediment in contact with lake water may be retained at around 3°C throughout a year, while boundary temperature between the debris and the dead ice is kept exactly at the freezing point. The dead ice may be melt by conductive heat flow through the sediment and the debris.

After lake ice has disappeared at the end of April, lake water absorbs solar radiation at the surface and the surface layers in less than around 15 m are quickly heated up during the pre -monsoon season from May. The heating continues until early June just before melting season and warms up to around 40 m in depth. As a great amount of meltwater flows into the lake during the monsoon season, the layers from 10 m to 40 m in depth are cooled by the intrusion of cold water from the glacier. In September near the end of melting season, the clear thermocline appears at around 15 m in depth. As air temperature continuously decreases and falls down below melting point at mid-October as well as the decrease of solar radiation, water temperature also decreases monotonously. The lake starts to be frozen from the shore in early November and the surface is entirely covered by ice possibly in early December. In February when the ice thickness reaches maximum thickness of around 50 cm, clear thermocline could appear in the upper layer in less than 10 m in depth, since the upper layer is cooled enough.

Horizontal distributions of the water temperature profile are shown in Figs. 32-a and -b, respectively obtained on 25 June, 1994 and on 3 November, 1994 at the points # 0 to # 5 in Fig. 13. Except for the points # 0 and N # 0, the profiles in June (Fig. 32-a) indicate similar distributions with a difference of less than 1 °C at equivalent depths. The profiles at # 0 and N # 0, both near the glacier terminus, exhibit a great temperature change at around 40 m in depth. The source of cold water below this depth will be discussed in Section 7.5.4.1. The profiles in November (Fig. 32-b) indicate that the isothermal surface layers are made up due to the wind mixing and cooling, with a slight difference in temperature along the lake longitudinally. These seasonal variations in temperature are related to heating and cooling at the surface and dynamic behaviors of lake water. Further studies should be conducted in view of the lake hydrodynamics for understanding how to develop such thermal structure.

7. 5. 1. 2 Water Temperature at the Lake Surface

With the objective of collecting the basic data for a long wave radiation in a heat balance study at the lake surface, water temperature at the lake surface was continuously measured in the resolution of 0.1 °C during the period from the end of June to the beginning of November, 1994.

A time series of surface water temperature measured at the point # 5 is shown in Fig. 33. The extremely large diurnal variation but relatively small daily fluctuation with a daily average of 5-6

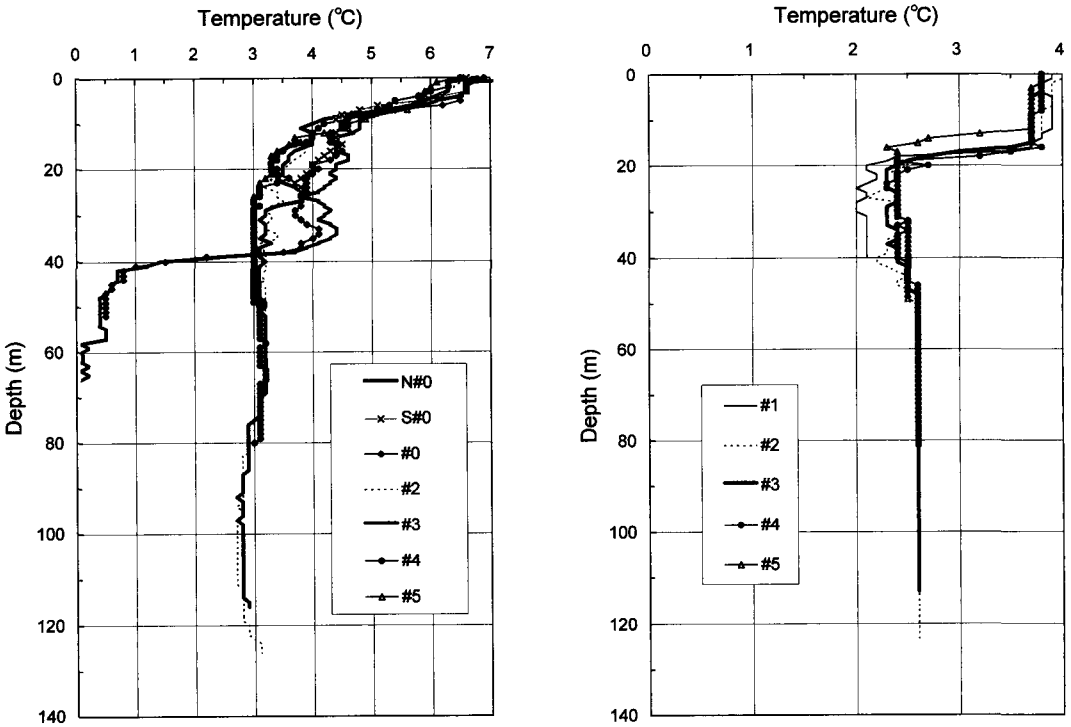

Fig. 32 : Vertical profiles of water temperature along the center line of the lake : a) June, 1994. b) November, 1994.

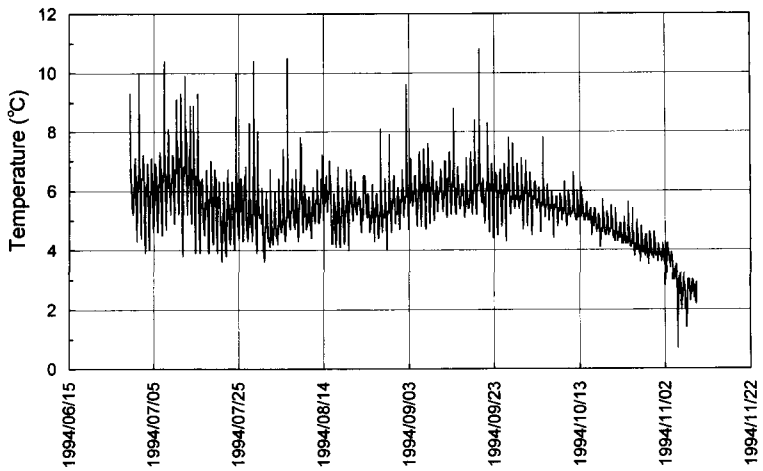

Fig. 33 : Seasonal variation of water temperature on the lake surface measured at the point # 5.

°C are seen during the monsoon season. The daily average starts to decrease from early October with decreasing diurnal amplitude.

7. 5. 1. 3 Water Temperature of Outflow at the Outlet

Water temperature at the outlet was measured to estimate the heat loss from the lake. Due to the topographical characteristics of the drainage basin, almost all the surface waters in the Tsho Rolpa basin, not only meltwater but also rainwater, are once absorbed into the Trakarding glacier system. Thus water with freezing point is supplied into the lake. Since only around 20-40 L/s of water is supplied into the lake as a surface stream as mentioned in Section 7.1.9, temperature of almost all the supplied water can be regarded to be at freezing point. Discharge at the outlet, Q, with temperature, T, may lose the heat energy of cQT from the lake, where c is specific heat of lake water. Water temperature was measured in almost one year from late June, 1994 to late May, 1995.

The water temperature shows clear daily and seasonal variations as shown in Fig. 34 corresponding to the variation of air temperature (Fig. 18) and solar radiation (Fig. 21). The daily amplitude is larger in summer than in winter. The water temperature is comparable to or slightly lower than air temperature during the monsoon season, but higher in dry season when air temperature decreases below freezing point. Even in the winter season water temperature shows above 1° C because of the enough heat storage in the lake during summer and the insulation from cooling by the thick ice cover in winter. While the water temperature during the rainy season exhibits an almost constant value of 4.5 to 5.5°C, it drastically decreases during October to mid-November from around 5°C to around 2.5°C due to the abrupt decrease of air temperature and solar radiation. Accordingly, with the decrease of discharge to a minimum in the next mid-March, water temperature also reaches a minimum of around 1°C and then rapidly increases after lake ice melts away which may occur in the end of April.

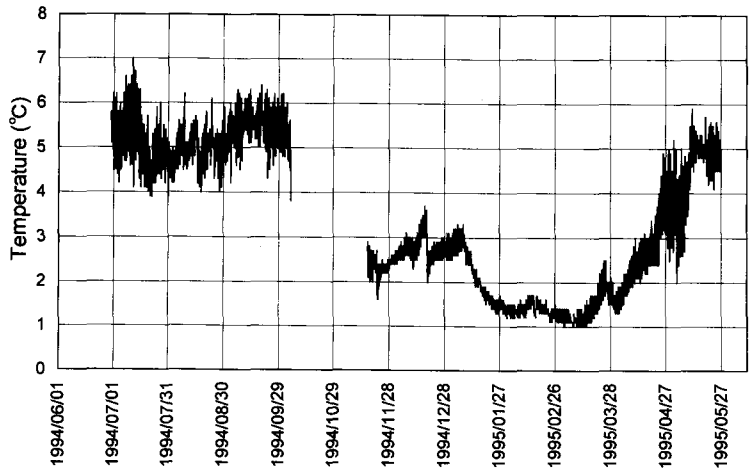

Fig. 34 : Seasonal variation of water temperature at the outlet.

It is evident that the outflow water is slightly cooler than the lake surface water in comparison Fig. 33 with Fig. 34 during the end of June to the middle of October. This is because the lake surface is heated by solar radiation but the outflow water partially includes deeper cold water of the lake.

7. 5. 2 Albedo of the Lake Surface

Albedo of the lake surface was measured in the condition of surface water SSC (suspended particle concentration) of 157 mg/L in June, 1994 at the point # 5 (see Fig. 13) including fine, cloudy and rainy period at the same point as the measurement of surface water temperature. Solar elevation at the time when albedo was observed is calculated. The relationship between albedo, α, and solar elevation, h, in degree is shown in Fig. 35. The empirical equation derived is expressed as $\alpha = 0.785h^{-0.451}$. The value of albedo was the order of some 0.15 in average during daytime.

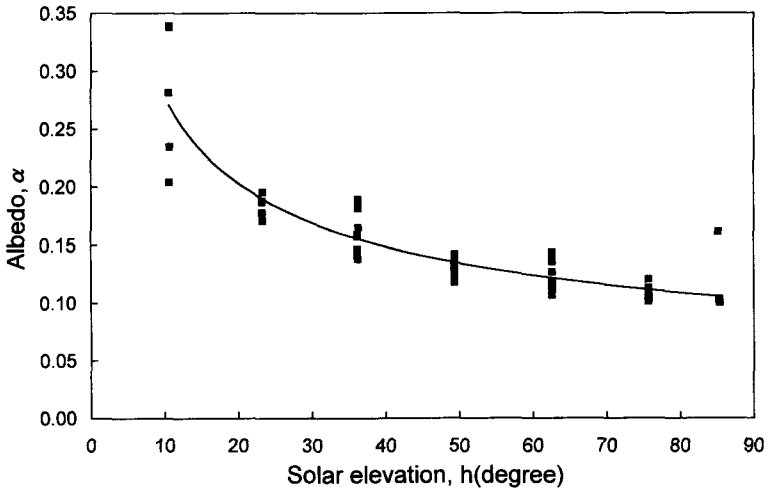

Fig. 35 : Relationship between albedo and solar elevation.

7. 5. 3 Annual Cycle of the Thermal Regime on the Lake

The thermal regime of the lake is characterized by the limited period of heat absorption in lake water. As the results of heat balance study of the lake (Sakai and Yamada, 1997), lake water is mainly heated up by solar radiation in the pre-monsoon period between late April, just after lake ice formed during cold winter season melting away and open water exposed under sun shine, and mid-June, just before the heavy melting season coming. Solar radiation is the main heat source for lake water : other heat balance terms are negligibly small throughout a year. Lake water stores the great amount of heat during pre-monsoon period, then monotonously loses the stored heat in the other seasons.

Though the hot summer season provides a lot of heat to lake water by relatively strong solar radiation, a great deal of meltwater (0℃) supplied into the lake considerably contributes to cool lake water enough. This situation starts from mid-June and continues to late September by the time when solar radiation decreases and air temperature falls below freezing point. The lake starts to

freeze in early November and is completely covered by ice by late November. Ice thickness increases more than 50 cm by the end of next March (Kadota, 1994). From late September through winter lake water is warm enough comparing with surrounding climate. Lake water surely loses stored heat in one-sided. Lake ice starts to melt in early April and completely disappears by late April (personal communication with Dr. T. Kadota). Stored heat in the lake is minimized in this season.

7. 5. 4 Suspended Particles in the Lake

Transparency of lake water is less than 10 cm because of high turbidity due to fine suspended particles. If a hand is inserted vertically into the lake to the wrist, the finger tips are not visible.

Since the suspended particles in lake water might strongly influence the physical properties of the lake, suspended particle concentration (SSC mg/L), its particle size distribution, sedimentation rate and particle size distribution of bottom sediment were investigated at various points in the lake in various seasons.

Water was sampled by the Van Dorn - type water sampler and its turbidity was measured by Turbidity Meter of light transmission type. The turbidity was converted into SSC obtained by filtering the sampled water with an opening of 0.45μmm.

7. 5. 4. 1 Source of Suspended Particles

There are two sources of the suspended particles ; one is turbid water pouring into the lake from the en-glacial mouth(s) of Trakarding glacier and the other is the lateral moraines inducing almost incessant collapse as seen clearly in Photo 24.

As shown previously in Fig. 32-a, the sharp discontinuity in water temperature was found at the depth of ca. 40 m at the points # 0 and N # 0 in June, 1994. At the same time, SSC measurements were made at N # 0. In fact, as shown in Fig. 37 in next Section, SSC abruptly changed from 260 mg/L at a depth of 40 m to 900 - 1200 mg/L below 50 m. This clearly indicates that cold (0°C) and highly turbid water flows into the lake through the en-glacial mouth(s) and occupies the lower layer below 40 m. The mouth is probably situated in a locally limited position because such a cold and highly turbid water was found at only two points among the five points observed transversally along the glacier terminus. According to the result of depth sounding near the glacier terminus, a bottom channel can be detected ; a rope or a string suspending a sensor was often inclined downstream -ward during the observations. Unfortunately, the size of the channel was not observed but surely more than at least 10 m in depth and a few ten meter in width.

The cold and turbid water supplied from the glacier included relatively coarse suspended particles as shown in Fig. 39-d of Section 7.5.4.3.

7. 5. 4. 2 Vertical Profiles of Suspended Sediment Concentration and Bulk Density

The vertical profiles of SSC were obtained in the various seasons at around the deepest point as shown in Fig. 36. The SSC increases almost linearly with depth in any season, while the vertical profile slightly fluctuates seasonally. Absolute value of SSC clearly increases from June to

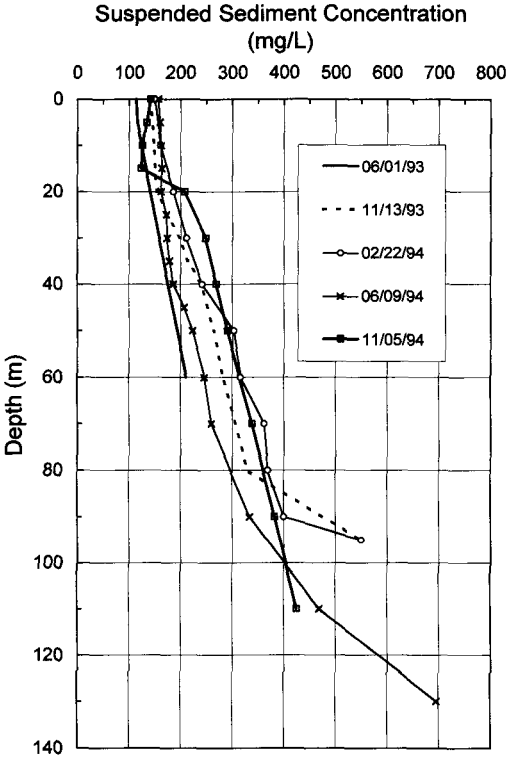

Fig. 36 : Seasonal variation of the vertical profile of suspended sediment concentration (SSC) at around the deepest point.

November. SSC may increase during the monsoon season due to the relatively great supply of turbid water from the glacier and moraine materials supplied by collapse of the lateral moraines. During winter and before melting season, considerable net deposition of suspended particles on the lake bottom could occur because of a very little water inflow and no active collapse of the frozen lateral moraines. Thus SSC gradually decreases during winter and then is retrieved to the level of previous June after the start of the melting season.

The horizontal variation of SSC profile is shown in Fig. 37. The profiles were measured in June, 1994 at the points N # 0, # 2 and # 3 and November, 1994 at # 0, # 2, # 3 and # 5 (see Fig. 13). The profile in June shows a clear difference from point to point but those in November indicate no remarkable difference. The unique SSC distribution at the point N # 0 is already discussed in just the previous Section. Those horizontal variations may be understood by considering seasonal variations in lake dynamics and the seasonal supplying processes of suspended particles.

Though the density of pure water is determined by only water temperature, bulk water density of the lake is considerably influenced by suspended particles. The bulk density ρ_ω is calculated by the following equation :

$$\rho_\omega = (1 - C \cdot 10^{-6}/\rho_s)\ \rho_\theta + C \cdot 10^{-6},$$

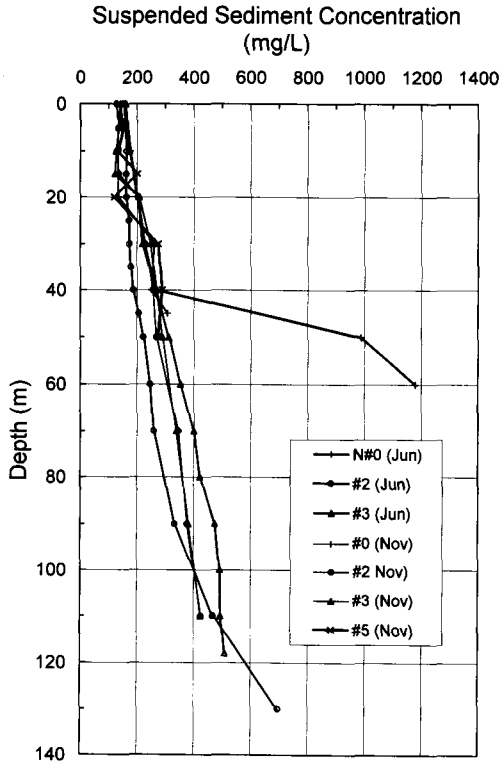

Fig. 37 : SSC profiles measured longitudinally along the lake in June and November, 1994.

where C is a SSC in mg/L, ρ_s is the particle density in g/cm^3 and ρ_θ is the pure water density at temperature of θ°C. Since water temperature was simultaneously measured with SSC, the density profile was easily calculated. The particle density ρ_s was assumed to be 2.65 g/cm^3.

The bulk density profiles are shown in Fig. 38. The profile patterns are quite similar to those of Fig. 36 because the bulk density ρ_ω is strongly influenced by SSC. The bulk density thus exhibits a monotonous increase with depth throughout a year, irrespective of the large seasonal fluctuations of water temperature in the layers less than 50 m in depth as shown in Fig. 31. It should be noted that the stable stratification of lake water throughout a year is remarkable characteristics of high turbid lake. Suspended particles act as the obstacle of water convection in the lake. The stable stratification through all the seasons puts us one question : How can the heat stored in the surface layers be transported to the lake bottom to keep temperature almost constant around 3°C ? The bottom water is considered to be cooled by dead ice melting. Such heat transport may need wind -driven action of lake water since a heat source to melt the dead ice beneath the lake bottom is only the surplus of heat balance at the lake surface, which is mainly given by solar radiation. The dynamic processes of lake water may be the key to understand the heat transport from surface to the bottom.

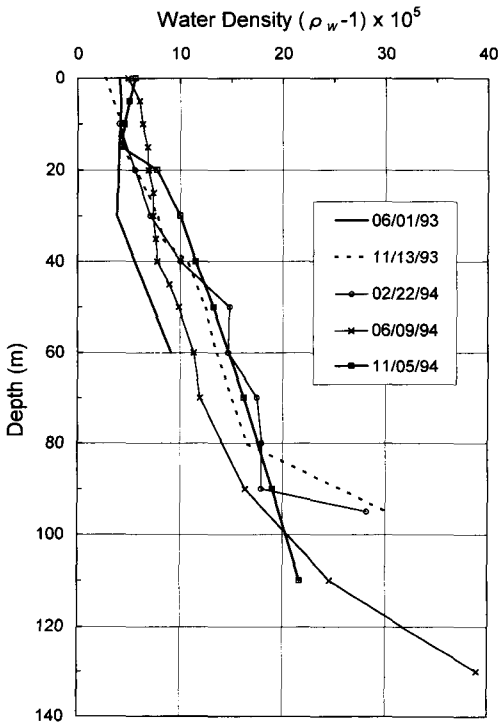

Fig. 38 : Seasonal variation of the vertical profile of bulk density.

7. 5. 4. 3 Size Distribution of Suspended Particles

A seasonal variation of particle size distribution with depth is shown in Figs. 39-a to -d. Figure 39-a was obtained at around the deepest point on 26 June, 1994 ; Fig. 39-b and -c around the lake center at the point # 3′, on 13 November, 1993 and on 22 February, 1994, respectively. Figure 39-d was obtained at the point N # 0 on 27 June, 1994, where the profiles of water temperature and SSC were simultaneously measured as already shown in Figs. 32-a and 37.

The particle size distributions are shown as relations between particle size in phi scale and frequency percent (wt. %) of each size fraction. The phi scale is defined as $\psi = -\log_2 d$, where d is a particle diameter in mm. This scale means that the larger the-value the smaller the particle diameter. The particles with the diameter of 2 mm ($\psi = -1.0$) to 1/16 mm ($\psi = 4.0$) are defined as *sand*, those with 1/16 mm to 1/256 mm ($\psi = 8.0$) as *silt* and those smaller than 1/256 mm (or larger than 8 in ψ) as *clay*.

Suspended particles mostly consist of silt and clay. This indicates that sand and more coarser particles are settled out on the lake bottom immediately, because their settling velocity is too large to be suspended in water. At the end of June when much meltwater is supplied into the lake, as shown in Fig. 39-a, the lake has a distinct two-layer structure such as the upper clay-rich and silt -poor layer above 40 m in depth and the lower clayey silt layer below 40 m. This structure may be retained during the heavy melting season in the monsoon period when many suspended particles are

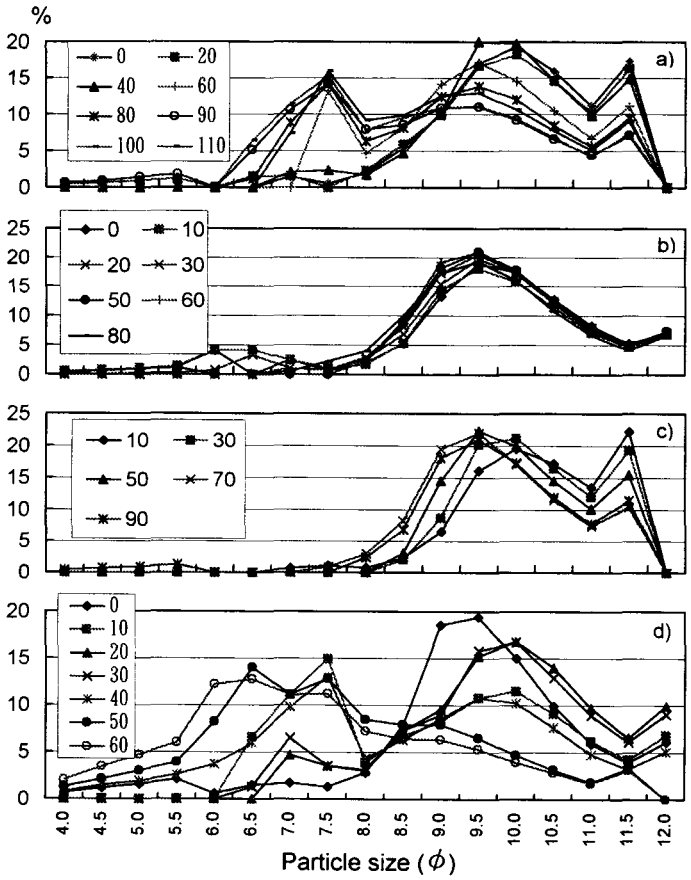

Fig. 39 : Size distribution of suspended particles at various depths :
a) at the point # 2, around deepest point measured in June, 1994 ;
b) at the point # 3', near mid-lake in November, 1993 ;
c) at the point # 3' in February, 1994 ;
d) at the point N # 0, near the glacier terminus in June, 1994.

supplied into the lake. At the end of November when air temperature falls below freezing point and the particle supply diminishes, the two layer structure disappears and almost the same distribution patterns can be seen through all the depth as shown in Fig. 39-b. In the ice-covered period, as shown in Fig. 39-c, relatively coarse particles in the upper layer are easily settled down to the deeper layer, so that the upper the layer the finer the particles.

The particle size distributions near the glacier terminus show complex features with depth as shown in Fig. 39-d. Most of the particles in the layers above 40 m are clay or silty clay, which is the similar to those at around the deepest point (Fig. 39-a). This suggests that the size distributions in the upper layer at N # 0 are determined by the advective sediment diffusion induced by wind -driven currents (Chikita et al., 1997) (see Figs. 23 and 24). The particles at the depths of 50 m and 60 m are clayey silt with a small amount of sand. These coarse particles were clearly supplied by sediment-laden underflow, a kind of density currents, originating from the en-glacial mouth(s).

Suspended particles in outflow water at the outlet consist almost of clay ($\psi > 8$) as shown in Fig. 40-a, since coarse particles are settled out on the lake bottom on the way to the outlet. In the leakage water flowing out on the outer slope of the end moraine (x marks in Fig. 16), the size distribution is similar to that at the outlet as shown in Fig. 40-b. It suggests that leakage water does not come from the melt of the dead ice buried in the moraine but from lake water directly.

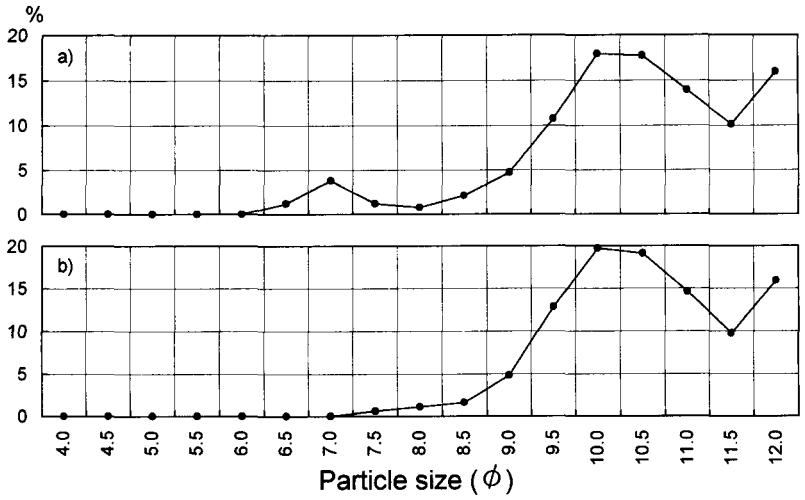

Fig. 40 : Particle size distribution of
a) outflow water at the outlet ;
b) leakage water.

7. 5. 5 Bottom Sediment of the Lake

The bottom sediment was sampled at the points # 1 to # 5. At # 1, only a few gravel were taken out from the bottom. No bottom sediment was found. That may be due to not enough time to cause sedimentation after this area is converted to become the lake, or the existence of too strong underflow coming from the glacier to accumulate particles of sand, silt and clay. In fact, lake water velocity of about 0.5 m/s was measured at the bottom layer near the glacier terminus (personal communication with K. Chikita, Hokkaido University). The sediment of the other points consists of sand, silt and clay as shown in Fig. 41-a. The sampling points # 1 to # 5 are approximately located at 0.5 km, 1 km, 1.5 km, 2 km and 2.5 km far from the glacier terminus, respectively as shown in Fig. 13. As far away from the glacier terminus, the ratio of sand and coarse silt ($\psi \leqq 5$) decreases and that of the fine silt and clay ($\psi > 6$) increases. It is a distinct characteristics that the medium silt of $5 < \psi \leqq 6$ is very poor or lack in the bottom sediment at all the points. It is evident that the sediment sorting occurs according to the distance from the glacier terminus. Since the sedimentation of sand and coarse silt almost disappears in between the points # 4 and # 5, the considerable sediment sorting is terminated in between 2 to 2.5 km from the glacier terminus.

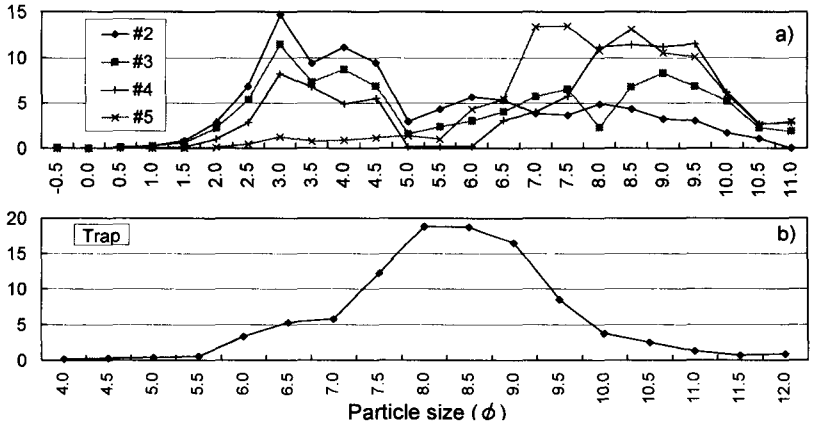

Fig. 41 : Particle size distribution of
a) bottom sediment at the points # 2 to # 5 ;
b) sediment trapped near the bottom of # 5.

7. 5. 6 Sedimentation Rate

Suspended particles are continuously deposited on the lake bottom. The sedimentation rate (g/cm^2) was measured by fixing cylindrical sediment traps with the diameter of 10 cm near the bottom of the point #5 during 8 to 13 November, 1993. The daily sedimentation rate is observed as 6.18×10^{-3} g/cm^2. Since the vertical profiles of SSC do not show great seasonal and horizontal variation as shown in Figs. 36 and 37, the annual sedimentation rate at the point #5 could be estimated as 2.26 g/cm^2. If this rate can be adopted over the lake basin with the area of 1.39 km^2, the annual amount of deposit is derived to be of the order of 3×10^4 ton over the lake basin. Since higher sedimentation rate is expected near the glacier terminus area due to sedimentation by the sediment-laden underflow, the annual amount of total deposit in the lake basin is expected to be actually larger than the above value.

The annual amount of suspended particles in the inflow water is estimated to be at least of the order of 10×10^4 ton, since SSC of inflow water is more than 1000 mg/L as mentioned in Section 7. 5.4.1 and the annual water discharge through the outlet was already estimated as the order of 100 million m^3 which is exactly equivalent to the annual inflow from the glacier. The sediment supplied from the lateral moraines and the unnamed glacier should be taken into account. The latter is, however, negligibly small. The former is estimated to be of the order of 1×10^4 ton if the surface area of the lateral moraine collapsing is assumed as 450,000 m^2 ; its rate of erosion is annually of the order of 1 cm ; the density of the moraine itself is about 2 g/cm^3. SSC of the outflow water at the outlet is less than 200 mg/L. Thus annual sediment loss from the lake is evaluated as less than 2×10^4 ton. Finally annual net balance of suspended particles is evaluated to amount to more than $(11-2) \times 10^4$ ton. It brings an average deposit of 6.5 g/cm^2 or about 3.2 cm in thickness over the lake bottom of 1.39 km^2 in area.

The annual amount of deposit, 2.26 g/cm^2 obtained from the sediment trap at the point # 5 is too small compared with 6.5 g/cm^2 obtained above. This indicate that nearer the glacier more the deposition. Large deposition of suspended particles as well as sand / coarse silt particles may not be made in uniform but occur higher rate in the uplake area.

The particle size distribution of sediment trapped at the point # 5 is shown in Fig. 41-b. The sediment $\psi = 6.0$ to 11 in size is dominant with unimodality. This distribution pattern is reasonably similar to that of bottom sediment at # 5 as shown in Fig. 41-a. Note the phi scale in Fig. 41-b is different from that in Fig. 41-a.

7. 6 Chemistry of Water, Snow and Ice Related to Tsho Rolpa

In order to obtain the basic information on the chemical background of the lake and around the lake, water samples were collected in June and July of 1994 and their chemistry was examined. The samplings were made from the lake water, pond water on the Trakarding glacier, snow in the accumulation area of the Trambau glacier, a supra-glacial stream water on the Trambau glacier, Trambau glacier ice, outflow water at the outlet, leakage water form the end moraine, rainwater in the rain gauge installed on the Instrument Island and river water of Rolwaling Khola and Tama Kosi. The ionic concentrations, electric conductivity and pH were measured in the laboratory. The results are shown in Table 7.

It is evident that precipitation in this area is relatively acidic but ionically pure with low electric conductivity (EC). Lake water is relatively rich in HCO_3^-, Ca^{2+} and SO_4^{2-}, and also relatively high in EC with a value about 40 μS/cm. This is common to outlet water, leakage water and river water. That is probably because terrestrial materials with ions rich in HCO_3^-, Ca^{2+} and SO_4^{2-} induce the waters with such ionic concentration and high value of EC.

The ion of PO_4^{3-} is not traced in all the samples and NH_4^+ concentration is very poor except in the pond water, snow, dead ice and rainwater. The lake and river waters are near neutral at pH of 6.4 to 6.9, while the other samples indicate a slightly acidic property.

7. 7 Present Growth Rate of the Lake

Tsho Rolpa has been continuously growing since about 45 years ago as discussed in Section 6. 3.3. The lake expands in the longitudinal direction owing to the retreating of the glacier and also deepening by virtue of dead ice melting. The lake has no space to expand for the lateral direction, since both the sides of the lake confined by the lateral moraines. Present growth rate is discussed in this Section.

The longitudinal growth of the lake is not due to melting of the cliff-shaped terminus but rather due to the collapse of the cliff, i. e. calving as mentioned in Section 7.1.5. The calving results in the lake growing upstream-ward. Survey of the contact line between the lake and the terminus of Trakarding glacier is practically difficult because it is not possible to approach the glacier terminus, either from the lake side or from the unstable glacier side without incurring very high risks. Therefore, the photographs of the contact line had been taken from the left side bank. As shown in Photo 34, the contact line has shifted upstream year after year. The growth rate of the lake is

Table 7 : Chemical composition of water, snow and ice related to Tsho Rolpa.

	Sampling Point	Depth m	EC μS/cm	pH	Cl mg/l	NO_3 mg/l	PO_4 mg/l	SO_4 mg/l	Na mg/l	NH_4 mg/l	K mg/l	Mg mg/l	Ca mg/l	HCO_3 mg/l
Pond Water	Trakarding Glacie	0	19.9	6.12	0.90	0.43	0.00	1.38	0.79	0.12	1.56	0.06	1.76	6.71
		1	21.5	6.06	0.89	0.31	0.00	1.29	0.83	0.48	1.39	0.08	1.56	7.31
		2	14.3	5.84	0.32	0.64	0.00	1.20	0.34	0.04	0.75	0.06	1.46	4.82
		3	13.0	5.85	0.18	0.47	0.00	1.15	0.23	0.00	0.71	0.06	1.31	4.82
		4	13.0	5.85	0.17	0.31	0.00	1.25	0.23	0.00	0.74	0.04	1.25	4.76

	Sampling Point	Depth	EC μS/cm	pH	Cl mg/l	NO_3 mg/l	PO_4 mg/l	SO_4 mg/l	Na mg/l	NH_4 mg/l	K mg/l	Mg mg/l	Ca mg/l	HCO_3 mg/l
Surface Snow	Trambau Glacier	5400 m	4.0	5.21	0.23	0.15	0.00	0.00	0.19	0.03	0.13	0.02	0.06	2.38
		5800 m	10.5	5.15	0.43	0.56	0.00	0.28	0.37	0.39	0.26	0.04	0.47	2.42
		5900 m	2.9	5.30	0.08	0.06	0.00	0.00	0.06	0.00	0.02	0.01	0.09	2.54
		5700 m	3.9	5.91	0.15	0.17	0.00	0.00	0.12	0.06	0.07	0.01	0.17	4.76
Supra-glacial Stream Water	Trambau Glacier		15.2	4.69	0.09	0.00	0.00	2.83	0.23	0.00	0.40	0.13	1.57	1.54
Glacier Ice	Trakarding Glacier		18.5	5.75	1.43	4.06	0.00	0.00	0.14	0.00	0.92	0.03	0.28	4.16
Fossil Ice	Unnamed Glacier left bank of lake	4800 m	11.0	6.59	1.28	0.00	0.00	0.00	1.09	0.24	0.62	0.00	0.10	16.38
Seepage Water	End Moraine		38.9	5.61	0.07	0.00	0.00	3.69	0.57	0.00	1.28	0.23	5.86	3.44
Rainwater	Instrument Island		7.5	5.61	0.16	1.20	0.00	0.24	0.14	0.32	0.17	0.02	0.43	3.52
			8.6	4.05	0.49	0.76	0.00	0.21	0.39	0.35	0.36	0.00	0.20	0.00
			5.7	5.46	0.33	0.42	0.00	0.00	0.27	0.26	0.26	0.00	0.07	3.18
Lake Water	Outlet		39.2	6.69	0.08	0.00	0.00	3.60	0.55	0.00	1.32	0.33	6.08	16.56
River Water	Rolwaling Khola	Na	46.1	6.59	0.13	0.00	0.00	3.19	0.53	0.00	1.14	0.20	7.90	20.68
	Rolwaling Khola	Beding	40.8	6.61	0.08	0.00	0.00	3.14	0.51	0.00	1.06	0.20	6.80	18.08
	Tamba Kosi	Jagat	36.1	6.65	0.22	0.00	0.00	1.69	0.76	0.00	1.01	0.19	5.36	17.28
	Tamba Kosi	Singati	36.8	6.68	0.48	0.14	0.00	1.65	0.98	0.00	1.56	0.33	4.87	17.06

EC : Electric Conductivity

	Point	Depth m	EC μS/cm	pH	Cl mg/l	NO_3 mg/l	PO_4 mg/l	SO_4 mg/l	Na mg/l	NH_4 mg/l	K mg/l	Mg mg/l	Ca mg/l	HCO_3 mg/l
Lake Water of Tsho Rolpa	#940602	0	40.1	6.37	0.10	0.00	0.00	3.95	0.60	0.00	1.35	0.33	6.83	17.08
		5	40.4	6.51	0.15	0.14	0.00	3.98	0.65	0.00	1.41	0.29	6.96	16.88
		10	43.4	6.52	0.56	0.86	0.00	4.06	0.95	0.00	1.65	0.34	7.03	16.66
		15	41.1	6.27	0.20	0.00	0.00	4.05	0.69	0.00	1.39	0.28	7.05	16.88
		20	41.7	6.68	0.19	0.21	0.00	4.04	0.68	0.00	1.45	0.29	6.94	17.04
		25	41.0	6.86	0.14	0.00	0.00	4.00	0.64	0.00	1.45	0.31	6.93	20.82
		30	40.8	6.69	0.14	0.00	0.00	3.92	0.66	0.00	1.36	0.31	7.05	17.30
		35	41.9	6.70	0.24	0.00	0.00	4.05	0.74	0.00	1.46	0.31	7.09	17.24
		40	40.6	6.59	0.15	0.00	0.00	3.91	0.66	0.00	1.53	0.31	6.68	16.58
		45	39.9	6.51	0.13	0.00	0.00	3.63	0.63	0.00	1.43	0.28	6.65	16.54
		50	39.7	6.36	0.13	0.00	0.00	3.60	0.65	0.00	1.37	0.25	6.19	16.14
		60	39.1	6.48	0.10	0.00	0.00	3.38	0.55	0.00	1.41	0.27	6.05	16.48
		70	39.5	6.58	0.13	0.00	0.00	3.41	0.58	0.00	1.34	0.27	6.39	16.68
		90	39.7	66.0	0.13	0.00	0.00	3.19	0.56	0.00	2.00	0.19	6.03	17.42
		110	40.3	6.58	0.09	0.00	0.00	3.18	0.56	0.00	1.57	0.24	6.17	17.58
		130	42.5	6.57	0.23	0.24	0.00	3.27	0.69	0.00	1.71	0.25	6.36	18.14

	Point	Depth m	EC μS/cm	pH	Cl mg/l	NO_3 mg/l	PO_4 mg/l	SO_4 mg/l	Na mg/l	NH_4 mg/l	K mg/l	Mg mg/l	Ca mg/l	HCO_3 mg/l
Lake Water of Tsho Rolpa	#940600	0	40.0	6.44	0.13	0.00	0.00	3.82	0.61	0.00	1.40	0.21	6.21	16.14
		10	38.0	6.57	0.14	0.15	0.00	3.32	0.54	0.00	1.26	0.26	6.21	15.92
		20	40.0	6.58	0.17	0.00	0.00	3.53	0.63	0.00	1.45	0.23	6.31	16.66
		30	39.3	6.56	0.12	0.00	0.00	3.50	0.58	0.00	1.44	0.22	6.24	16.80
		40	39.0	6.60	0.15	0.23	0.00	3.09	0.60	0.00	1.53	0.23	6.34	16.76
		50	34.7	6.50	0.16	0.00	0.00	2.70	0.67	0.00	1.98	0.30	4.77	15.18
		60	34.1	6.56	0.13	0.00	0.00	2.58	0.66	0.00	1.95	0.27	4.68	15.20
		65	47.6	6.49	0.11	0.00	0.00	2.91	0.68	0.00	2.38	0.34	7.76	21.20

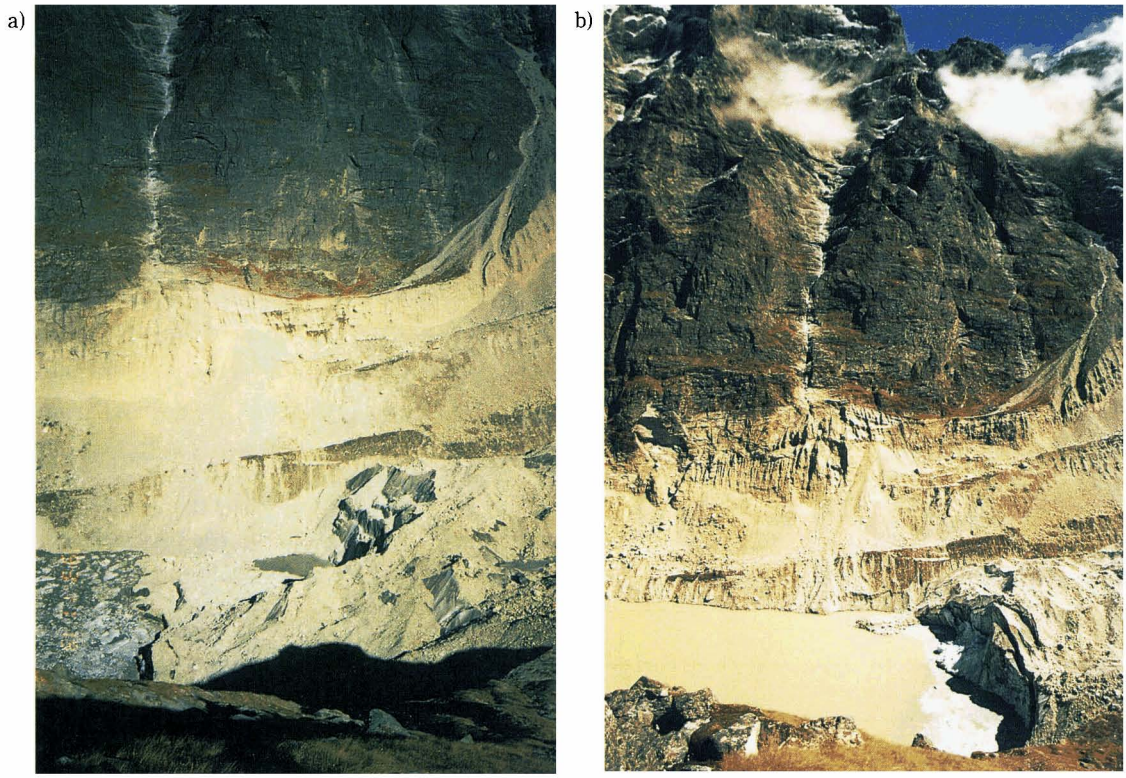

Photo 34 : Expansion of the lake and retreat of the glacier due to calving : a) 19 November 1993. b) 4 October 1995.

estimated at some 200 m during about 2 years from 19 November, 1993 (Photo 34-a) to 4 October, 1995 (Photo 34-b), which was obtained by surveying the positions of characteristic landmarks such as cracks on the bedrock, talus etc. on the right side bank behind the contact line ; annual growth rate is roughly estimated as 100m. Since the lake was born 45 years ago and has grown to 3.2 km in length so far, the average annual rate of expansion is about 70 m, so that recent growth rate may be rather accelerated.

As discussed by Chikita et al. (1997), active calving may be caused by the effective melting of the cliff-root at the glacier terminus due to wind driven surface current of well warmed water. Surface water warmed by solar radiation is drifted to the cliff-shaped glacier terminus by the up-valley wind during daytime.

The deepening rate of the lake can be measured by depth measurements at the fixed points or fixed lines set out in the lake. It is theoretically easy but practically not possible except in the areas near the end moraine and islands due to the difficulty of positioning the fixed points and of re-measuring the depth at the same point, because the lake shores at the lateral moraines are very risky to approach. The lake is bounded on both sides by the loose and unstable lateral moraines with considerably steep slopes (Photo 24), which is collapsing almost continuously into the lake, especially in summer monsoon season. The glacier terminus is also very dangerous due to its calving.

One can not find any such fixed points in the lake except only in the winter season when the lake becomes covered by thick ice.

Due to the above limitations, the depth profiles were measured along a fixed line between Lama Island and Middle Island as illustrated by dashed line in Fig. 16. The depth profiles indicate that the deepening is still occurring as shown in Fig. 42 and the deepening rate of 48.1 cm in average through the measurement line is obtained during the period from 14 November, 1993 to 3 October, 1995. It corresponds to the annual deepening rate of 25.5 cm. The islands are confirmed to be also sinking into the lake due to the melting of dead ice beneath the islands.

The measured deepening rate between islands is rather small as compared to that at the deepest point as discussed in Section 6.3.3. That is because the debris acting as a effective heat insulator is thicker near the downlake area than at the deepest point. The significant fact derived from the deepening rate measurements establishes that, beyond doubt, the lake bottom is still deepening.

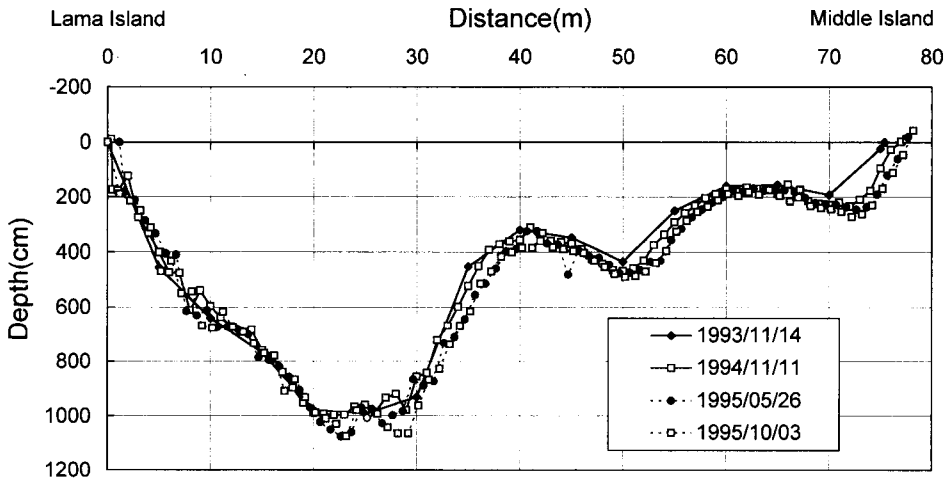

Fig. 42 : Deepening of the lake by means of bottom melting along the survey line shown by the dashed line in Fig. 16.

7. 8. Investigation of a Supra-glacial Pond as an Embryo of a Glacier Lake

Supra-glacial lakes have developed from ponds on the glacier. The present physical status of the ponds and their change with the lapse of time are essentially important for understanding the quick development mechanism of such glacier lakes. The ponds on the Trakarding glacier located near the glacier terminus were inspected on June, 1994. Seven ponds were found within 1.5 km from the glacier terminus with different color and turbidity due to the difference in their age and existing condition. At the pond chosen as typical among them, observations were conducted on the size and depth of the pond, water temperature of the pond surface, vertical profiles of water temperature, suspended sediment concentration and electric conductivity. The pond had unfortunately disappeared due to draining out through some crack(s) in the ice body constituting the pond basin when re

-measurement was attempted in October, 1994. For the convenience of future investigations, only meaningful data are shown here.

The pond is located a few hundred meters upstream of the glacier terminus and surrounded by exposed ice-wall with the area of 4075 m^2. The maximum depth is measured to be 9 m and the average is roughly estimated as 5.5 m and the water stored in the pond is calculated to be 22,400 m^3. There were no visible surface flows into and out of the pond.

During the observation period from 19 to 23 June, 1994, the pond level increased almost linearly by 31 cm, which corresponds to 316 m^3 of meltwater in the daily average supplied into the pond through the en-glacial channel(s). The change in the volume of water during those 4 days is equivalent to 5.6 % of total water stored in the pond. Since the temperature of supplied water into the pond is assumed to be at freezing point, it could considerably affect the thermal regime of the pond.

The surface temperature of the pond is shown in Fig. 43. In comparison with the surface temperature of Tsho Rolpa (see Fig. 33), which is around 6°C, it shows a remarkably low value of 3.5±2 °C because of much inflow of meltwater with freezing point and also the cooling effect of glacier ice under and surrounding the pond. The temperature profiles at the deepest point is shown in Fig. 44 ; average water temperature through depth increased from 3.3°C on 20 June 12 : 46 to 3.4°C on 23 June 14 : 30. During this period, heat balance of the pond is evaluated by assuming the pond to be rectangular in shape, uniform ice melting to occur over the pond bottom and the heat received in the pond immediately to be consumed by ice melting. The heat balance is evaluated to be positive from the meteorological data concurrently obtained. Daily melting rate of 5.5 cm is estimated. If the rate retains through the hot summer season for about 4 months, 6.6 m of bottom ice may be melted out. The real melting rate should be directly measured to validate the above melting rate and assumptions. The mechanism of heat transfer to the pond bottom should also be studied by further investigation. It is, at least, clarified that a pond is an effective heat absorber.

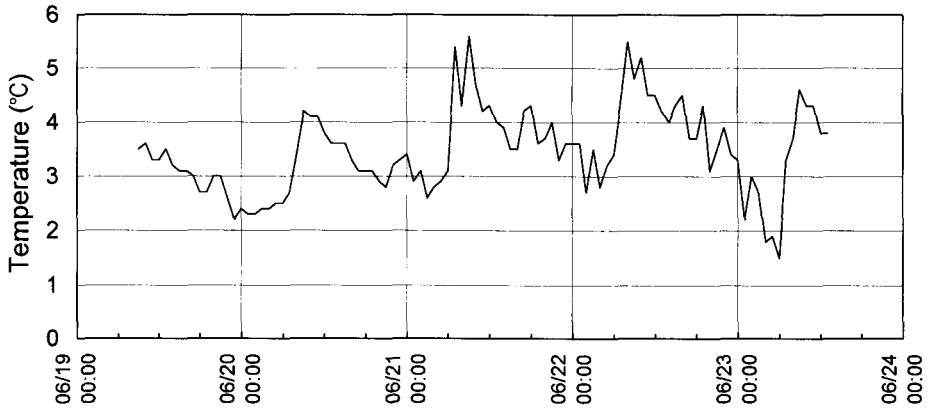

Fig. 43 : Surface water temperature of a pond on the Trakarding glacier.

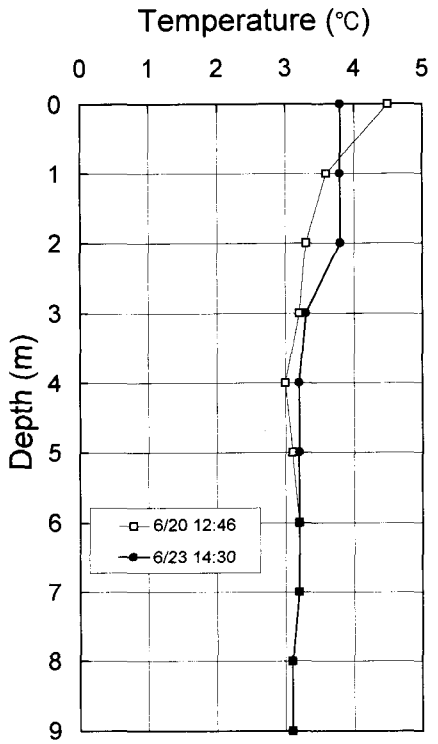

Fig. 44 : Vertical profiles of water temperature of the pond on the Trakarding glacier.

The profiles of suspended sediment concentration (SSC) measured in the pond are shown in Table 8 as an example for future reference. The value of SSC is remarkably less than that of Tsho Rolpa. Thus bulk density rather depends more on water temperature but less on SSC, which derives active convection and then effective heat transfer from the surface to the bottom.

Table 8 : Vertical profile of suspended sediment concentration in pond water of the Trakarding glacier.

Depth (m)	0	1	2	3	4	5	5.3 (bottom)
Turbidity (mg/L)	18.8	18.4	17.8	17.4	17.0	17.2	16.5

As mentioned in Section 6. 3. 5, if a pond lasts long enough and some thermal regime goes beyond the critical condition, a pond starts to grow up wider and deeper to become a supra-glacial lake. Existence of water with free surface on the glacier drastically changes the thermal condition of the glacier surface. It can absorb more heat than that on the debris covered surface.